

Regional climate model sensitivities to parametrizations of convection and non-precipitating subgrid-scale clouds over South America

Stefan Lange · Burkhardt Rockel · Jan Volkholz ·
Bodo Bookhagen

Received: 21 January 2014 / Accepted: 22 May 2014 / Published online: 18 June 2014
© Springer-Verlag Berlin Heidelberg 2014

Abstract This study provides a first thorough evaluation of the Consortium for Small scale MOdeling weather prediction model in CLimate Mode (COSMO-CLM) over South America. Simulations are driven by ERA-Interim reanalysis data. Besides precipitation, we examine the surface radiation budget, cloud cover, 2 m temperatures, and the low level circulation. We evaluate against reanalysis data as well as observations from ground stations and satellites. Our analysis focuses on the sensitivity of results to the convective parametrization in comparison to their sensitivity to the representation of non-precipitating subgrid-scale clouds in the parametrization of radiation. Specifically, we compare simulations with a relative humidity versus a statistical subgrid-scale cloud scheme, in combination with convection schemes according to Tiedtke (Mon Weather Rev 117(8):1779–1800, 1989) and from the European Centre for Medium-Range Weather Forecasts Integrated Forecasting System (IFS) cycle 33r1. The sensitivity of simulated tropical precipitation to the parametrizations of convection and subgrid-scale clouds is of similar magnitude. We show that model runs with different

subgrid-scale cloud schemes produce substantially different cloud ice and liquid water contents. This impacts surface radiation budgets, and in turn convection and precipitation. Considering all evaluated variables in synopsis, the model performs best with the (both non-default) IFS and statistical schemes for convection and subgrid-scale clouds, respectively. Despite several remaining deficiencies, such as a poor simulation of the diurnal cycle of precipitation or a substantial austral summer warm bias in northern Argentina, this new setup considerably reduces long-standing model biases, which have been a feature of COSMO-CLM across tropical domains.

Keywords South America · COSMO-CLM · Clouds · Convection · Precipitation · Radiation

1 Introduction

Since the beginning of dynamical atmospheric modeling and despite many efforts, the deficiencies in the representation of cloud processes in climate models have remained a source of much uncertainty in climate projections (Randall et al. 2003; Stocker et al. 2013). This is because clouds significantly influence thermodynamic and hydrological budgets, but need to be parametrized in mesoscale models (Tompkins 2002).

A variable intimately related to clouds and of paramount importance for climate impact research is precipitation. In light of climate change, questions related to the hydrologic cycle are: Where do humans have to adapt to changes in water availability (Parry et al. 2007; Liersch et al. 2012; Schewe et al. 2014)? Are extreme rain events going to be more frequent or intense (Marengo et al. 2009; Toreti et al. 2013; Fischer et al. 2013a)? How will ecosystems such as

S. Lange (✉) · J. Volkholz
Potsdam Institute for Climate Impact Research, Potsdam,
Brandenburg, Germany
e-mail: slange@pik-potsdam.de

S. Lange
Department of Physics, Humboldt University, Berlin, Germany

B. Rockel
Institute of Coastal Research, Helmholtz-Zentrum Geesthacht,
Geesthacht, Schleswig-Holstein, Germany

B. Bookhagen
Department of Geography, University of California,
Santa Barbara, CA, USA

the Amazon rainforest respond to changes in precipitation patterns (Salazar et al. 2007; Cook et al. 2011; Warszawski et al. 2013)?

The deficiencies of parametrizations of cloud processes are reflected in, among other things, precipitation biases. Particularly in the tropics, convection is an important process in this respect and its parametrization has received much attention (e.g. Betts and Jakob 2002; Bechtold et al. 2004; Santos e Silva et al. 2012). However, since convection involves many coupled processes between the surface, the planetary boundary layer, and the free troposphere (Bechtold et al. 2004), the quality of its representation in climate models depends on several other model components as well.

In this study, we focus on the parametrization of non-precipitating subgrid-scale clouds. Such clouds significantly affect radiative fluxes and thereby also influence convective processes and precipitation (Hohenegger et al. 2008). Strong sensitivities of precipitation to the parametrization of radiative processes have been found, most notably in tropical regions (Xu and Small 2002; Morcrette et al. 2008).

For the typical resolution of mesoscale models, subgrid-scale clouds exist due to fluctuations of temperature and humidity within a grid cell. Traditionally, there have been two approaches to their parametrization (Tompkins 2002). One class of schemes relates cloudiness to relative humidity (RH, e.g. Slingo 1987), with cloud cover being a monotonically increasing function of RH, which is zero at some critical RH and one at grid-scale saturation.

The second approach is of statistical nature (e.g. Sommeria and Deardorff 1977) and assumes a certain probability-density function type for the subgrid-scale distributions of temperature and humidity. By linking the moments of the distributions to other processes such schemes facilitate a more physically consistent representation of clouds. The statistical scheme implemented in the model used in this study assumes Gaussian distributions, which are centered around the grid-scale values and whose variances are estimated by the turbulence parametrization.

Our primary goal is to assess the importance of the representation of subgrid-scale clouds in an atmospheric model for a faithful simulation of precipitation. To that end we need to put this specific model sensitivity in relation to others. We choose the well-known sensitivity of precipitation to the parametrization of convection as a reference.

The analysis of more variables than just precipitation is necessary, if we are to understand the differences between simulation results for different model setups. This calls for a comprehensive climate model evaluation. Since model sensitivities to cloud and convective processes can be expected to be greatest around the equator, we restrict our model experiments to a tropical domain.

To our knowledge, this is the first regional climate model (RCM) sensitivity study comparing a statistical to a RH subgrid-scale cloud scheme in combination with different convective parametrizations. Although we only present results for a specific RCM over a specific domain, our findings may benefit climate modeling wherever a faithful simulation of clouds and convection is key.

We use the RCM COSMO-CLM, which features the introduced parametrizations of subgrid-scale clouds as well as different convection schemes. In the past, this model has mostly been run over Europe (e.g., Jaeger et al. 2008; Zahn and von Storch 2008; Hohenegger et al. 2009; Davin and Seneviratne 2011) but recent applications to East Asia (Fischer et al. 2013b) and Africa (Nikulin et al. 2012; Panitz et al. 2013) have been spurred by the COordinated Regional climate Downscaling EXperiment (CORDEX, Giorgi et al. 2009) initiative.

In order to accomplish two tasks with one effort, we conduct our sensitivity study over a region, where the model has not yet been thoroughly evaluated—South America. We follow the domain specification by CORDEX, thus simplifying possible future model intercomparisons and regional multi-model ensemble climate projections. COSMO-CLM performance studies over South America have so far been restricted to either the southern part of the continent (Wagner et al. 2011) or to the evaluation of precipitation as the only variable (Rockel and Geyer 2008). In the latter study, the model was run over several subregions of the globe using its standard mid-latitude setup and results were highly unsatisfactory in the tropics, where the model showed a sharp land-sea contrast of strong overestimation (underestimation) of rainfall over oceans (continents). The same model deficiency has recently been observed over Africa (Panitz et al. 2013) and has motivated the present study.

There has been a range of attempts to simulate the South American climate with other RCMs. While some studies focus on model evaluation (Nicolini et al. 2002; Seth and Rojas 2003; Solman et al. 2013), others provide regional climate projections based on greenhouse gas emission or land-surface change scenario runs of General Circulation Models (GCMs, Correia et al. 2008; Marengo et al. 2010, 2012a). We are going to relate our results from the COSMO-CLM evaluation to those of these models.

2 Climate, model, data, experiments

2.1 Climate of South America

The South American continent extends across several climate zones from 10°N to 55°S. Along its western shore, the Andes form a narrow but high orographic barrier

(Bookhagen and Strecker 2008). In line with climatological conditions, vegetation types vary considerably. While tropical South America is dominated by the vast Amazonian rainforest, various kinds of wood- and shrublands, savannas, and deciduous forests are found in the subtropics, and grasslands and semideserts prevail in southern South America.

Climatological phenomena that need to be captured are diversified. Throughout the year, the continent is framed by the Intertropical Convergence Zone (ITCZ) in the north, westerly winds in the south, and subtropical high pressure systems over the Pacific and Atlantic oceans in the west and east, respectively (Garreaud et al. 2009).

In austral winter, the ITCZ rain band retreats to northwestern South America, leaving the southern Amazon basin, the adjacent savanna, and northeastern Brazil in their dry season (Vera et al. 2006b; Liebmann et al. 2007). The westerlies carry extratropical cyclones to the south of the continent, supplying precipitation to the southwestern coast and to southeastern South America (SESA, Mendes et al. 2010).

In austral summer, the greatest part of the continent is subject to the South American Monsoon System (SAMS, e.g. Zhou and Lau 1998; Vera et al. 2006a; Marengo et al. 2012b). Next to the ITCZ, this comprises the South Atlantic Convergence Zone (SACZ), a band of moisture convergence and abundant precipitation extending south-eastward from central Amazonia (Nogués-Paegle et al. 2002; Carvalho et al. 2004). Further low-level features of the SAMS include a thermal depression called the Chaco low over northwestern Argentina and the South American Low Level Jet (SALLJ, Marengo et al. 2004), which transports large amounts of moisture from Amazonia to the subtropical plains through a narrow channel between the Andes and the Brazilian Plateau. The most prominent feature of the high level circulation is a large anticyclonic circulation called the Bolivian high, which can be considered together with the low level Chaco low as a response to the strong convective heating in the Amazon region. The SAMS is characterized by enhanced convective activity and heavy precipitation in tropical South America. The convection has a pronounced diurnal cycle, is frequently organized in squall lines or (mesoscale) convective systems, and is modulated by extratropical frontal systems (Molion 1993; Silva Dias et al. 2002; Rickenbach et al. 2002; Salio et al. 2007).

2.2 COSMO-CLM

The RCM COSMO-CLM or CCLM (COSMO model in CLimate Mode, Rockel et al. 2008) originates from the “Lokalmodell” of the German Weather Service (Steppeler et al. 2003), later on renamed as COSMO (CONsortium for

Table 1 Selected differences between convection schemes

	Tiedtke	IFS
Criterion deep convection	Moisture convergence	Cloud depth
Closure deep convection	Moisture convergence	Convective available potential energy
Turbulent entrainment	Constant	Decreases with height
Trigger test parcel ascent	From lowest level, with temperature perturbation	From several levels, with temperature and humidity perturbation
Precipitation efficiency	Constant	Decreases with vertical velocity, increases at low temperatures due to homogeneous freezing

Small scale MOdeling) model. In this study, simulations are performed with model version 4.25.3. CCLM is non-hydrostatic and is able to perform long-term simulations on highly resolved horizontal grids down to grid mesh sizes on the order of 1 km.

Lateral boundary forcing is applied according to the method of Davies (1976). We employ the ERA-Interim reanalysis data (Dee et al. 2011) for this purpose.

The cloud parametrizations distinguish between clouds at grid scale and at subgrid scale. A bulk water-continuity model describes the grid-scale clouds (Doms et al. 2011). It includes prognostic equations for water vapor, rain, snow, cloud liquid water and cloud ice.

Subgrid-scale clouds are considered as either stratiform, in which case they are treated as non-precipitating, or vertically extended, i.e. convective. For the latter type, two different parametrizations are available. The mass flux convection scheme by Tiedtke (1989) is the model’s default option. The scheme from the European Centre for Medium-Range Weather Forecasts (ECMWF) Integrated Forecasting System (IFS) cycle 33r1 as described by Bechtold et al. (2008) is the second option applied in the present study. In Table 1 we summarize the main differences between the schemes.

Characteristics of stratiform subgrid-scale clouds are taken into account in the parametrizations of turbulence and radiation. Two schemes are available for their diagnosis; one is statistical (Avgoustoglou 2011), the other one is based on grid-scale RH as proposed by Smagorinsky (1960), refined and extended by a simple cloud water parametrization by Geleyn and Hollingsworth (1979). We compare results with either approach utilized in the parametrization of radiation. In the turbulence parametrization we only employ the statistical scheme. The latter assumes Gaussian distributions for the saturation deficit and the liquid water potential temperature (Sommeria and Deardorff 1977; Mellor 1977), whose widths may be scaled

by the namelist parameter q_crit , for which Sommeria and Deardorff (1977) suggest a value of 1.6 and which we set to 1.5 as opposed to its default value of 4.0. For subsequent reference we note that the cloud cover fraction C of a grid cell is given by

$$C = C_s + (1 - C_s) C_c \quad (1)$$

with C_s and C_c being the contributions from stratiform and convective clouds, respectively. The former may be present due to grid-scale ($C_s = 1$) or subgrid-scale ($C_s < 1$) condensation. Irrespective of the employed convective parametrization, C_c is proportional to the cloud depth diagnosed by the convection scheme.

CCLM has the radiation transfer scheme by Ritter and Geleyn (1992) implemented. It is a delta-two-stream approximation of the radiative transfer equations with three spectral intervals in the solar and six in the thermal part of the radiation spectrum. In addition to the standard atmospheric gases the radiative properties of clouds (liquid and ice) and aerosols are taken into account.

Raschendorfer (2001) implemented a prognostic TKE-based scheme with a turbulent kinetic energy closure at level 2.5 according to Mellor and Yamada (1982) that includes effects from subgrid-scale condensation-
evaporation.

Soil processes are parametrized by the multi-layer soil model TERRA (Schrodin and Heise 2001). Plants are modeled following the biosphere-atmosphere transfer scheme approach by Dickinson et al. (1986). The bare surface is parametrized according to Dickinson (1984). In order to account for the deep roots in tropical rainforests, we lower the bottom of the deepest hydrologically active soil layer to 8 m (Nepstad et al. 1994; Baker et al. 2008).

2.3 Observational datasets

We employ site measurements and various gridded datasets for model evaluation. Prior to any comparison, the gridded data are interpolated from their native grid to the rotated geographical coordinate system of CCLM. In the case of radiative fluxes, cloud cover, and precipitation we apply a first-order conservative remapping scheme (Jones 1999).

Table 2 Locations, measurement heights, and temporal data coverages of LBA flux towers

	K34	K67	CAX	RJA	BAN
Longitude [°W]	60.21	54.96	51.46	61.93	50.16
Latitude [°S]	2.61	2.86	1.72	10.08	9.82
Height [m]	50.0	63.0	51.5	60.0	40.0
Coverage [y]	7	4	3	3	3

Temperature, geopotential height and winds are interpolated bilinearly. Winds are additionally rotated in order to account for the relative rotation of grids.

We evaluate precipitation against the Tropical Rainfall Measuring Mission (TRMM) 3B42 V7 daily satellite product from 1998 to 2011 at a native resolution of 0.25° (Huffman et al. 2007). It arguably is the best precipitation dataset available for tropical South America given its high resolution and the large uncertainties of gridded gauge measurement data, especially in Amazonia and along the Andes (Carvalho et al. 2012). The TRMM Precipitation Radar data only extend to 36°S but we do not consider this a problem since this study focuses on tropical climate and since inter-setup differences of modeled precipitation characteristics are small at more southern latitudes.

Total cloud cover is compared to the International Satellite Cloud Climatology Project (ISCCP) D2 monthly means from 1998 to 2007 which have a native resolution of 2.5° (Rossow and Schiffer 1999). The cloud cover estimates are based on satellite observations of infrared and visible radiation and have an uncertainty of about 5 %.

Surface shortwave and longwave net radiation are evaluated against the NASA-GEWEX Surface Radiation Budget (SRB) release-3.0 monthly estimates from 1998 to 2007 at a native resolution of 1° (Stackhouse et al. 2011), which are based on various input data including temperature and moisture profiles from the NASA Global Modeling and Assimilation Office GEOS-4 reanalysis product, and cloud parameters from ISCCP DX data. The estimates have uncertainties of about 20 W/m^2 for shortwave and 5 W/m^2 for longwave radiation.

2 m temperatures are compared to the Climatic Research Unit (CRU) TS3.21 monthly observations from 1998 to 2011 at the native resolution of 0.5° (Harris et al. 2013). This dataset covers land points only, but since CCLM employs the ERA-Interim sea surface temperatures (SSTs) we expect only minor differences of oceanic 2 m temperatures between different model runs.

Fields of geopotential height and wind at 850 hPa are evaluated against ERA-Interim reanalysis data. We also include ERA-Interim data in the evaluation of the above mentioned variables as a reference. Besides, this allows to identify biases introduced by the driving model.

In order to compare simulation results to site measurements at high temporal resolution we include data recorded at the towers of the LBA-ECO CD-32 Brazil Flux Network (Saleska et al. 2009). This dataset comprises hourly measurements from 9 sites in the years 1999 to 2006. However, for most sites this time frame is not entirely covered and at some of them the vegetation is non-natural which is a problem since the land cover data used by CCLM in the corresponding grid cells represent natural vegetation.

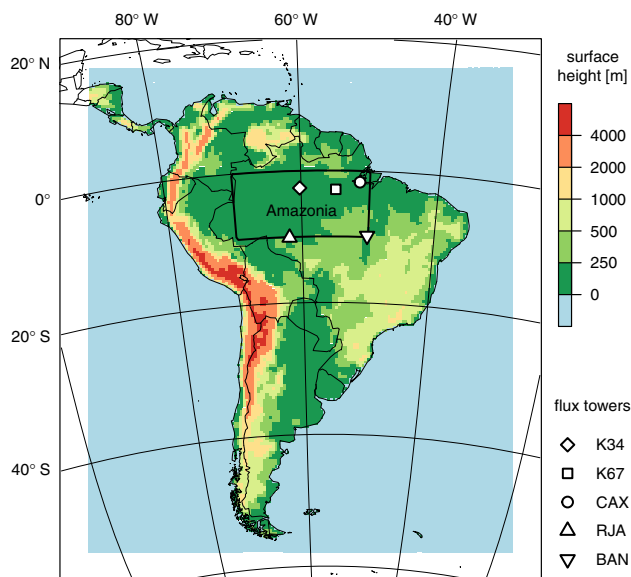


Fig. 1 Computational domain for CCLM simulations. The model evaluation is restricted to the CORDEX South America domain (colored). Marked are further the region we refer to as Amazonia in Sect. 3.2 (solid box) and the locations of the five flux towers, data recorded at which we employ in this study. Colors indicate surface height as it is represented in the model

Table 3 Abbreviations and schemes of CCLM setups

Setup	Convection scheme	Subgrid-scale cloud scheme
TR	Tiedtke	Relative humidity
TS	Tiedtke	Statistical
IR	IFS	Relative humidity
IS	IFS	Statistical

Choosing sites with natural vegetation only and providing at least 3 years of precipitation, temperature, and net radiation data, we ended up with the towers at Manaus Km34 (K34), Santarem Km67 (K67), Caxiuana (CAX), Reserva Jaru (RJA), and Bananal Island (BAN). Their location, measurement height, and temporal coverage is displayed in Table 2 (see also Fig. 1). All measurements were taken just above the canopy so that they may well be compared to the modeled surface fluxes and atmospheric variables at 2 m height. We compare tower measurements to data from the closest model grid cell, considering only times, when tower data are available.

2.4 Experimental setup

As previously mentioned, we evaluate CCLM simulations over South America with four different model setups, which differ in the chosen representations of convection (Tiedtke versus IFS scheme) and subgrid-scale clouds in the parametrization of radiation (RH versus statistical

scheme) but are otherwise identical. The labels of these 2×2 setups are displayed in Table 3.

The model is evaluated on the CORDEX South America domain, which implies a horizontal resolution of 0.44° . The computational grid includes 10 additional grid points on each side to abate boundary effects (Fig. 1). The vertical coordinate is set to have 40 levels reaching up to 30 km above sea level, and as suggested by Panitz et al. (2013) for tropical domains, we adjust the Rayleigh damping height to 18 km.

Our evaluation period covers 14 years from 1998 to 2011. Model runs are started in 1990 to allow for a spin-up of 8 years.

3 Results

In this section we first analyze seasonal mean values of precipitation, total cloud cover, 2 m temperature, surface shortwave, and longwave net radiation, as well as 850 hPa fields of geopotential height and wind. Second, our analyses focus on Amazonia with seasonal and diurnal cycles at the flux tower sites (cf. Fig. 1). We then evaluate the distribution of daily precipitation intensities and conclude with a comparison of mean cloud profiles as simulated with the different CCLM setups.

3.1 Seasonal mean values

3.1.1 Precipitation

We commence with the central variable of this study. Mean precipitation during austral summer (DJF) and winter (JJA) is shown in Fig. 2. In DJF, the TRMM and ERA-Interim data exhibit the typical monsoon season rainfall pattern with precipitation maxima along the ITCZ, the SACZ, and the eastern Andes (cf. Bookhagen and Strecker 2008).

The CCLM simulations show quite different qualities in reproducing this pattern. With the TR setup the model displays a bias contrast of more than 50 % overestimation over the oceanic part of the ITCZ and more than 50 % underestimation over land except along the Andes south of 20°S . Hence, the basic precipitation bias pattern over South America has not changed since Rockel and Geyer (2008). In fact, this land-sea bias contrast is a general deficiency of CCLM in the tropics as revealed by Rockel and Geyer (2008) and reported recently by Panitz et al. (2013) in model simulations over Africa employing the TR setup convection and cloud schemes.

Substituting IFS for Tiedtke convection smoothes rainfall patterns and reduces biases over land as well as over oceans. Especially the oceanic wet bias is almost completely removed and over the Andes the model produces

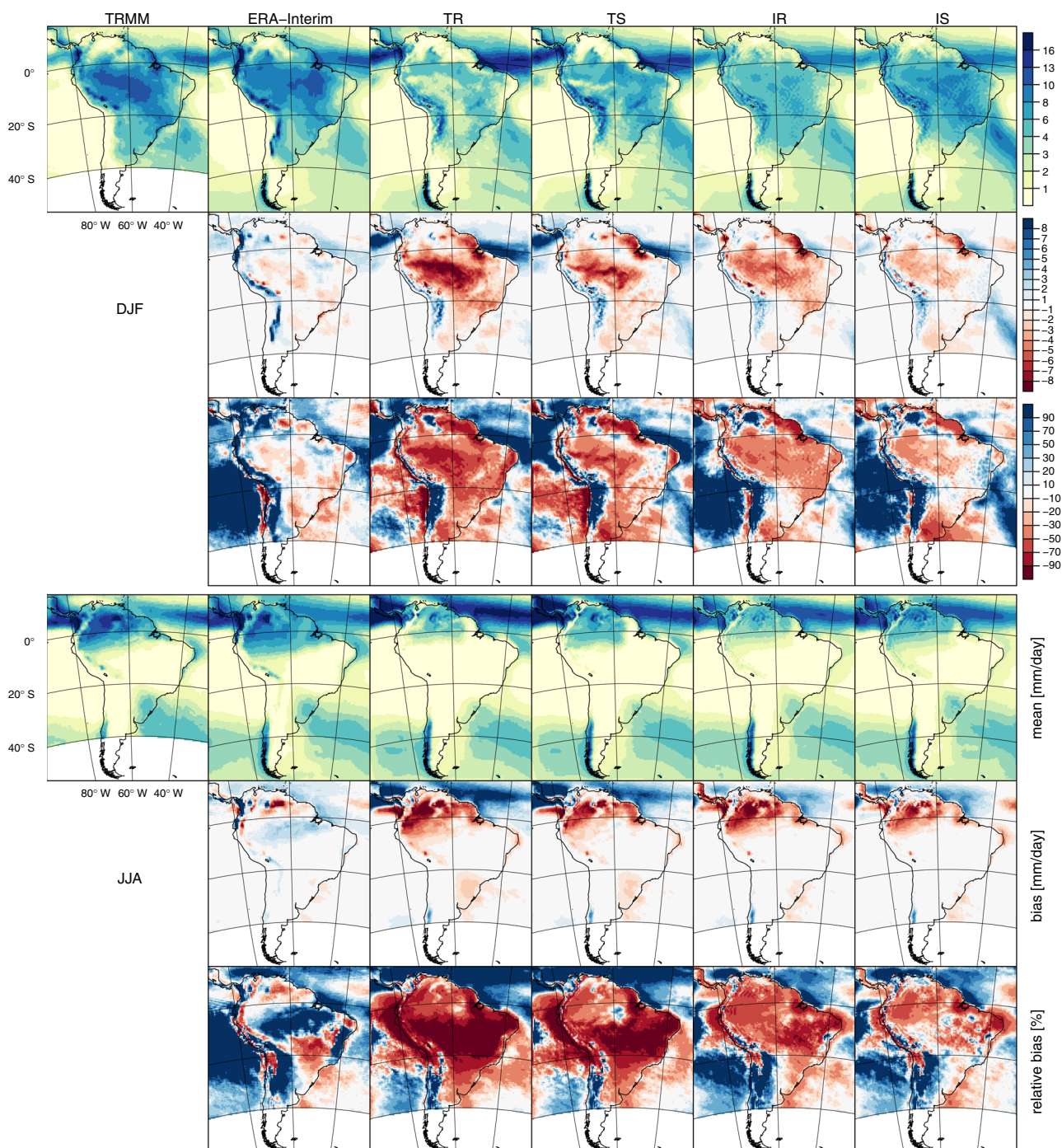


Fig. 2 Mean precipitation versus TRMM observations during austral summer (DJF, upper three rows) and austral winter (JJA, lower three rows) from 1998 to 2011. For each season, the top row shows the seasonal mean, the middle row shows the absolute (sim–obs), and the

bottom row the relative [(sim–obs)/obs] difference to the observation, which is displayed in the leftmost column, followed by ERA-Interim, and the CCLM simulations with the TR, TS, IR, and IS setup (from left to right)

less excessive precipitation. Gregory et al. (2000) found a similar smoothing of spatial rainfall patterns as well as rain rate reductions along the maritime ITCZ in global seasonal forecasts with the ECMWF IFS after changing the criterion for and closure of deep convection from those based on moisture convergence as proposed by Tiedtke (1989) to

ones based on cloud depth and convective available potential energy, respectively (cf. Table 1). Modifications of the scheme's trigger algorithm and entrainment rates led to qualitatively similar precipitation changes though (Bechtold et al. 2004). Since, moreover, the list of differences between the schemes presented in Table 1 is all but

complete (Bechtold et al. 2008), it is difficult to tell which differences are most responsible for the improvements seen in Fig. 2.

In comparison to simulations with the RH cloud scheme, those with the statistical scheme show a further reduced dry bias over land. With the IS setup the dry bias in western Amazonia is reduced to 30 %—a magnitude also found with other RCMs (Marengo et al. 2009; Solman et al. 2013); in eastern Brazil we see a mix of over- and under-estimations. While a major sensitivity of precipitation amounts to the convective parametrization could be expected, the large sensitivity to the cloud scheme is remarkable. We are going to elaborate on the latter below.

Some biases however, are common to all model setups and are also shared by other climate models. For instance, the overestimation of precipitation along the Andes (except its eastern slopes between 0° and 20°S) is a feature of ERA-Interim, the reanalyses CFSR and MERRA (Carvalho et al. 2012), and many RCMs (Marengo et al. 2009; Solman et al. 2013).

Another example is the dry bias of up to 50 % in northern Argentina, which is shared by all simulations while it is not seen in the ERA-Interim data, but observed in CFSR and MERRA (Carvalho et al. 2012). Observations have shown that monsoon-season rainfall is highly stochastic in this region and characterized by a heavy-tail distribution (Boers et al. 2013), which implies that heavy rain events (>20 mm/day) contribute considerably to the total precipitation. Some of these events are caused by the world's largest mesoscale convective systems (Vera et al. 2006a), which suggests that such systems are not well reproduced by the model. In Sect. 3.2.3 we show that CCLM strongly underestimates the frequency of heavy rain events. The particular importance of these events for the mean DJF precipitation over northern Argentina explains the dry bias.

Along the coast around the outlet of the Amazon river, the baseline land-sea bias contrast remains with all CCLM setups. It also is a feature of other climate models (Marengo et al. 2009; Solman et al. 2013; Joetzjer et al. 2013) and of the ERA-Interim. In CCLM, it might therefore result from inaccurate boundary conditions. In fact, ERA-Interim wind uncertainties in the Atlantic ITCZ are considerable as direct observations are essentially limited to satellite scatterometer measurements (Žagar et al. 2011) and since there is comparably little wind information in tropical mass field observations (Žagar et al. 2005). Findings by Bechtold et al. (2014) suggest that a better representation of the diurnal cycle of convection (cf. Sect. 3.2.2) could reduce the coastal bias contrast. Alternatively, one could attribute it to an interplay of an incorrect representation of the local land-sea circulation and a mischaracterization of the soil moisture-precipitation feedback: An erroneous land-sea

breeze circulation with too little rainfall over land dries out the soil. In reality this would lead to stronger convection over land (Taylor et al. 2012), which would counterbalance the model deficit, but with the two convection schemes employed here dryer soils inhibit convection (see Hohegger et al. (2009) for CCLM with the Tiedtke scheme and Taylor et al. (2012) for ERA-Interim with the IFS scheme). Presumably, the deficient simulation of this feedback also aggravates the aforementioned dry bias in northern Argentina.

In JJA, we see the same land-sea bias contrast as in DJF, which is again most pronounced for the TR setup and least for IS. Again, a swap of the convection scheme from Tiedtke to IFS reduces biases over land and oceans while a swap of the cloud scheme from RH to ST mainly yields increased precipitation over land. For the TR setup the SESA rainfall maximum is underestimated by up to 50 %, as by the RCMs in Solman et al. (2013). Moving from TR to IS, this bias declines gradually. For the IS setup, the modeled mean rainfall pattern resembles the TRMM observation. Remaining deficiencies include dry biases in northeastern Brazil and northern Amazonia, as well as wet biases in the Gulf of Mexico, in northern Argentina and Chile, all of which are also shared by ERA-Interim.

3.1.2 Total cloud cover

Since we observed a major sensitivity of modeled mean precipitation to the parametrization of subgrid-scale clouds, we also expect major differences in the modeled cloud cover between model setups. The DJF and JJA mean values of total cloud cover are shown in Fig. 3 and they indeed vary considerably between simulations. Compared to the ISCCP data, the TR setup generally yields too high mean cloud cover over the oceans in summer and winter. As could be expected, a change of the convection scheme results in smaller cloud cover changes than one of the parametrization of subgrid-scale clouds. With the IFS scheme, it is generally less cloudy than with the Tiedtke scheme. The IR setup yields the smallest overall biases in both seasons.

Substituting the statistical for the RH subgrid-scale cloud scheme yields increased (reduced) cloud cover in regions with frequent (rare) incidences of deep convection. This pattern of change is most clearly visible in DJF when we find a sharp boundary between these regimes approximately along a great circle through 10°S, 90°W and 30°S, 30°W. It suggests that the statistical scheme generates less subgrid-scale stratiform clouds, such that the total cloudiness is reduced in regions where stratiform clouds prevail, such as over the cool SSTs of the eastern Pacific (Mechoso et al. 2005). In regions with frequent deep convective activity we suppose that a more vigorous

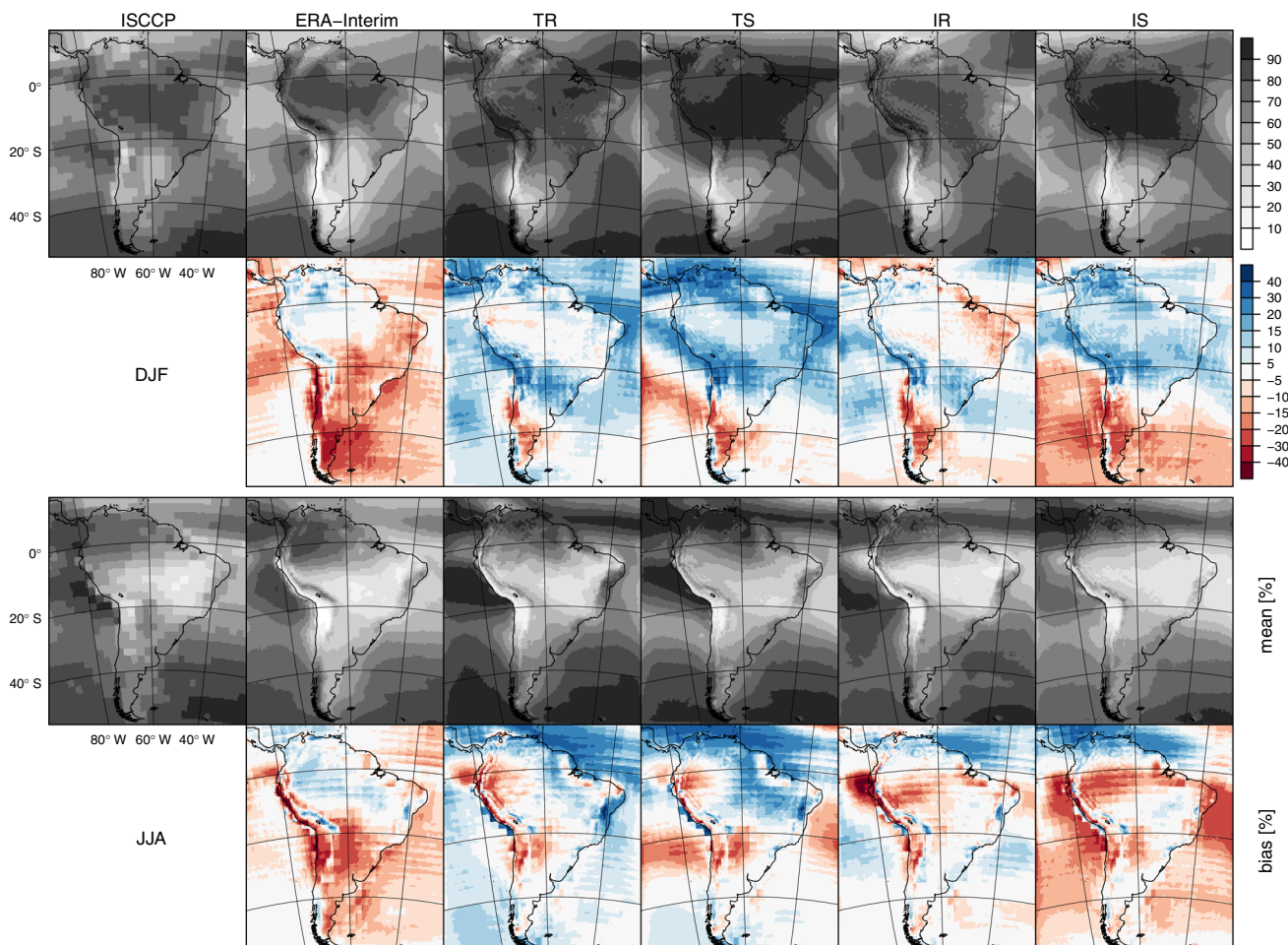


Fig. 3 Mean total cloud cover versus ISCCP observations from 1998 to 2007. Layout as described in Fig. 2, without relative biases

convective activity acts to counterbalance the by itself less frequent occurrence of stratiform clouds and leads to a greater overall cloudiness. This interpretation is consistent with the concurrently enhanced mean precipitation rates over Amazonia (cf. Fig. 2) and we are going to substantiate it below.

3.1.3 Surface shortwave net radiation

Since there is a direct relation between cloud cover and radiation budgets we investigate the latter in the following. The DJF and JJA mean values of net surface shortwave radiation are displayed in Fig. 4. Compared to the SRB estimates, the TR setup severely underestimates shortwave net radiation, especially over the oceans. Similar to precipitation, biases of the same kind and magnitude were found over Africa (Panitz et al. 2013).

Employing the IFS instead of the Tiedtke convection scheme considerably mitigates the biases, as does substituting the RH subgrid-scale cloud scheme. The differences between model setups are by far more pronounced over sea

than over land. With the IS setup the modeled shortwave net values resemble the SRB estimates in summer and winter. The remaining biases are underestimations (overestimations) inside (outside) the convergence zones ITCZ and SACZ.

The reduced surface shortwave net biases suggest a more correct representation of daytime clouds. As put forward by Morcrette et al. (2008), more solar radiation reaching the surface yields enhanced convection over tropical land masses. Thus, the continuous increases of surface shortwave net radiation from TR to IS are in line with the respective increases of precipitation over the South American continent.

Related to the consistency between different variables, we observe an odd situation north of 20°S (the equator) in austral summer (winter). In this area, a comparison of simulations with different parametrizations of subgrid-scale clouds shows a positive correlation of total cloud cover and net surface shortwave radiation. We discuss this apparent contradiction and provide a solution in Sect. 3.2.4.

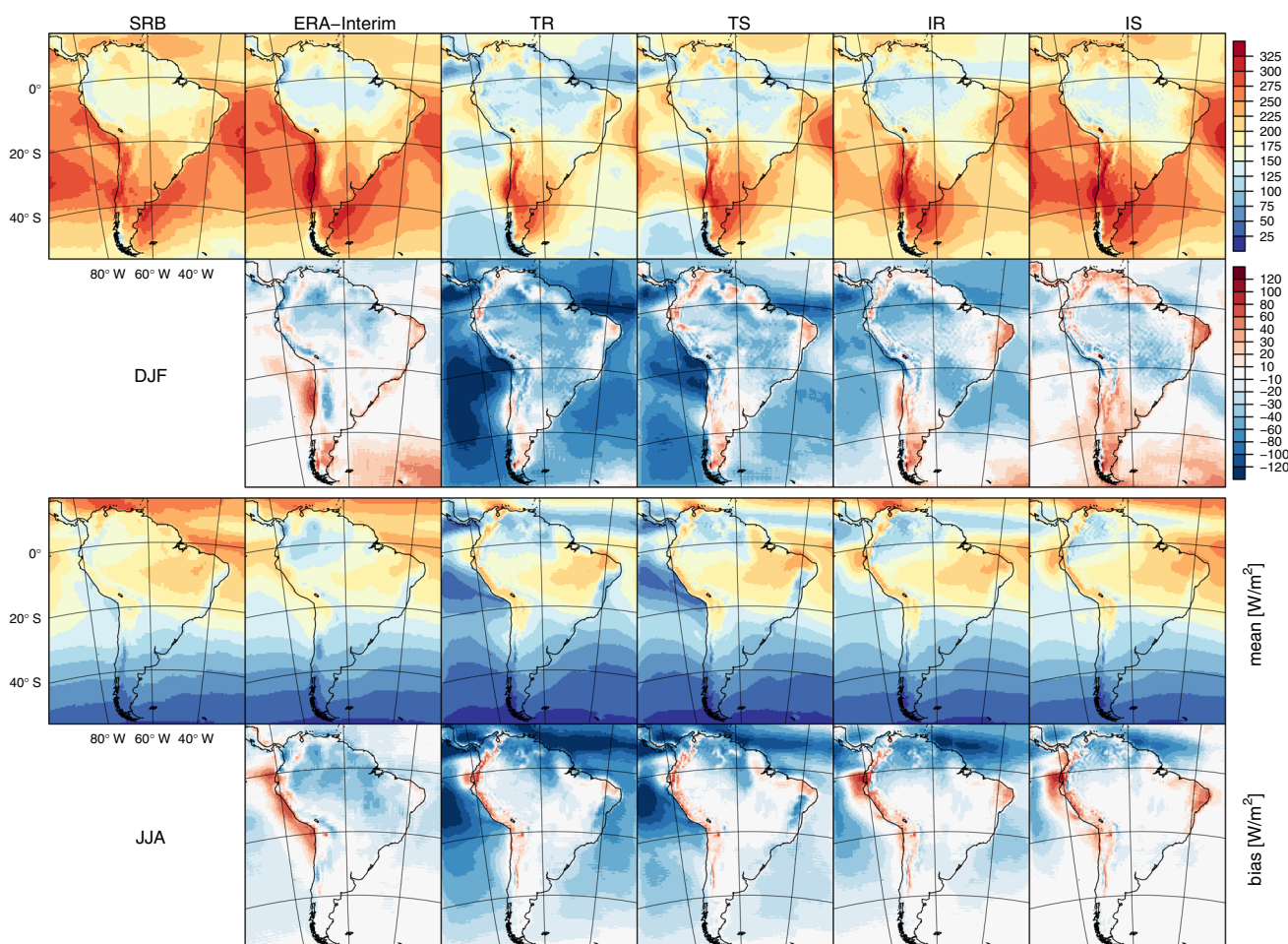


Fig. 4 Mean shortwave net radiation at the surface versus SRB observations from 1998 to 2007. Layout as described in Fig. 3

3.1.4 Surface longwave net radiation

In order to complete the radiation budget evaluation we now discuss DJF and JJA mean values of the modeled net surface longwave radiation (Fig. 5). Since the daytime radiation budget is shortwave dominated, longwave results primarily represent nighttime conditions. In comparison to the SRB data, the smallest biases are obtained with the IR setup.

Over land, using the IFS instead of the Tiedtke convection scheme mostly reduces biases while using the statistical instead of the RH subgrid-scale cloud scheme generally increases the outgoing longwave radiation, i.e. renders the net surface longwave radiation more negative, which leads to mixed bias changes.

Over sea, we observe increased outgoing longwave radiation for both, a swap of the convection scheme to the IFS, and a swap of the subgrid-scale cloud scheme to the statistical—with a greater sensitivity to the cloud scheme choice. With the IS setup, the outgoing longwave radiation is generally overestimated.

Considering the inter-setup differences of net surface shortwave and longwave radiation together, we conclude that with the statistical subgrid-scale cloud scheme the CCLM produces optically thinner clouds than with the RH scheme. For Amazonia in DJF, the validity of this conclusion is evidenced in Sect. 3.2.4.

3.1.5 2 m temperature

As an example of a variable which depends on the surface fluxes of radiation and precipitation, we evaluate the 2 m temperature, the DJF and JJA mean values of which are shown in Fig. 6. The bias patterns with respect to CRU observations are height corrected with a constant lapse rate of 0.65 K/100 m and do not differ much between model setups. In austral summer biases are greater than in winter.

All year round we find a cold bias in Amazonia, which we reconsider in Sect. 3.2.1 because of the discrepancies between CRU temperatures and those measured on the flux towers. Cold biases along the Andes and over the Guiana

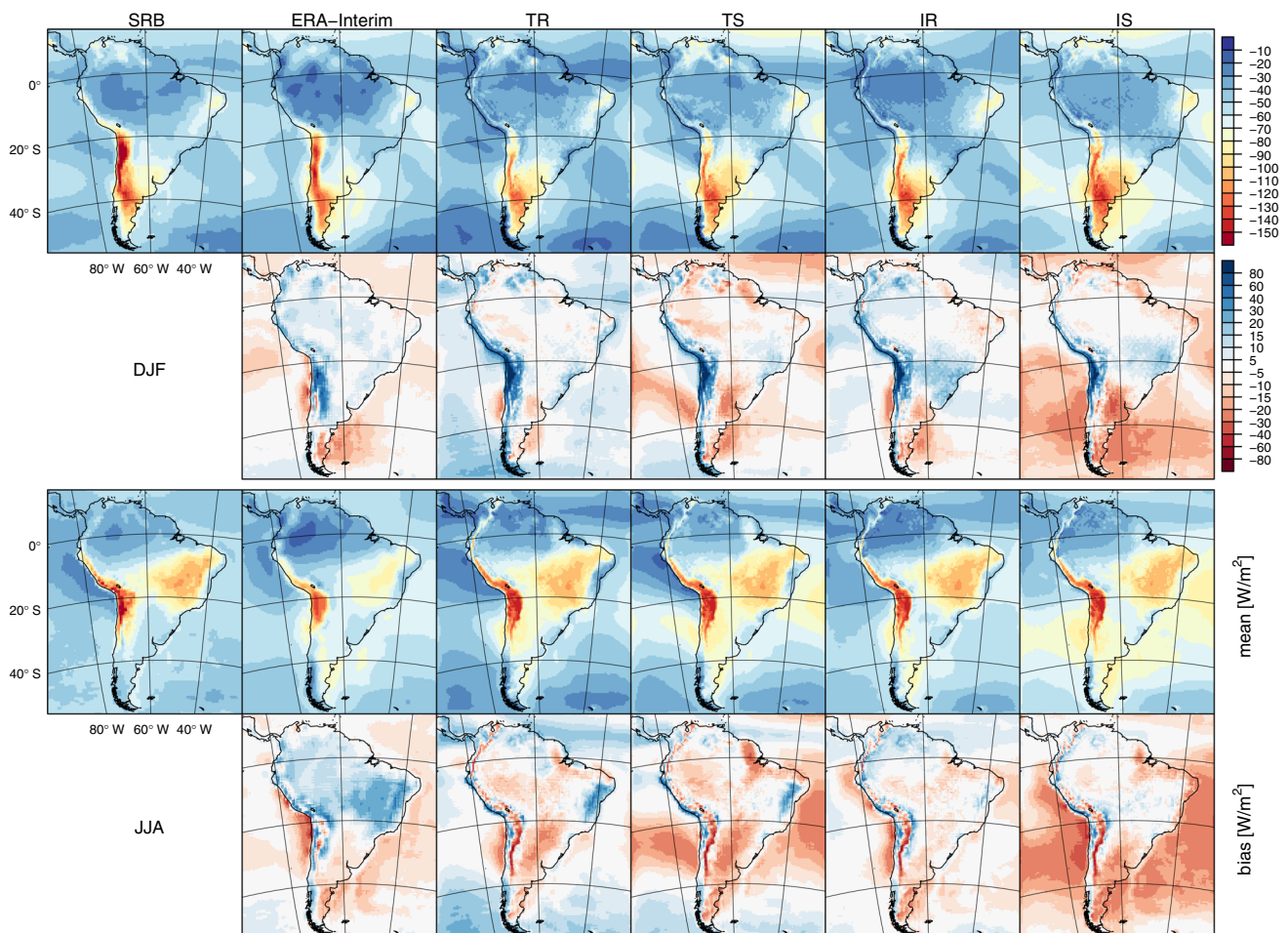


Fig. 5 Mean longwave net radiation at the surface versus SRB observations from 1998 to 2007. Layout as described in Fig. 3

highlands are mostly shared by ERA-Interim, as is a warm bias in the Atacama desert.

While CCLM mostly produces too low temperatures, we find a pronounced DJF warm bias in northern Argentina, which is common to many RCMs (Solman et al. 2013). In part, we attribute it to the severe dry bias in this region and season discussed in Sect. 3.1.1, since the respective precipitation and temperature biases significantly anticorrelate (99 % confidence level) across CCLM setups, and because the soil receives a lot of insolation in this area during summer (Fig. 4), which makes it susceptible to dry stress.

However, a linear regression reveals that the dry bias does not fully explain the warm bias. The work by Wagner et al. (2011) hints on its fundamental source being located outside the region of occurrence: The authors evaluated CCLM simulations over extratropical South America and found a substantial sensitivity of northern Argentinean DJF 2 m temperatures to the forcing data. Downscaling a GCM simulation, CCLM generated a warm bias of similar magnitude to the one found here. Yet, when forced by ERA40 reanalysis data, the model produced a slight cold

bias. Since the predominant DJF low level inflow to the region is from north, the warm bias might reflect modeling errors in the tropical part of the continent, possibly including a poor representation of the SALLJ. To check this hypothesis, we evaluate the 850 hPa circulation next.

3.1.6 Low level circulation

The DJF and JJA mean fields of geopotential height and wind at 850 hPa are displayed in Fig. 7. The ERA-Interim data show the westerlies in the south, the subtropical anticyclones over the Atlantic and Pacific oceans, the monsoon circulation in summer, and strong trade winds over the tropical Atlantic and northeastern Brazil in winter.

In DJF, CCLM generally exaggerates the relative strength of the Chaco low over northern Argentina, which leads to a regional bias cyclonic circulation that deflects the inflow of moist Amazonian air to the east. This probably contributes to the summer dry bias in the region.

Over western Amazonia, pressure is too high throughout the year and with all setups, which indicates too weak

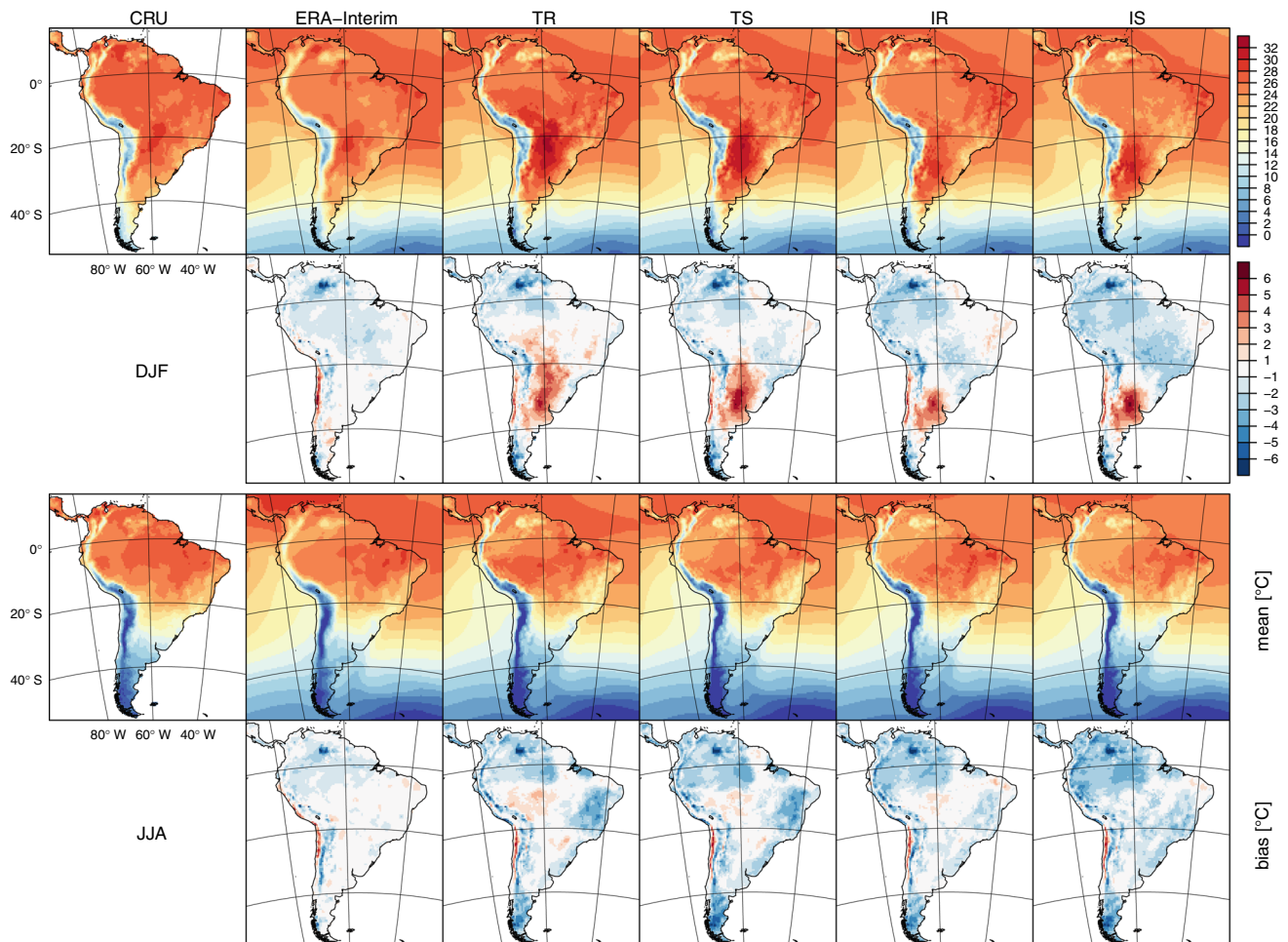


Fig. 6 Mean 2 m temperature versus CRU observations from 1998 to 2011. Layout as described in Fig. 3. Biases are height corrected with a constant lapse rate of 0.65 K/100 m

diabatic heating and is consistent with the underestimation of (convective) precipitation in this area (Fig. 2).

Generally, there is a strong dependence of pressure and circulation biases on the parametrization of subgrid-scale clouds. With the RH scheme, 850 hPa geopotential heights are mostly overestimated and we find an all-year bias anticyclone over the subtropical Atlantic as well as a bias antimonsoon circulation in DJF.

For simulations with the statistical subgrid-scale cloud scheme, the overall low level pressure and circulation biases are strongly reduced. In DJF, we find a bias cyclonic circulation over the subtropical Atlantic. It explains the northeast displacement and intensification (increased moisture convergence) of the respective SACZ rainband (Fig. 2).

Throughout the year and more pronounced with the IFS convection scheme, there is a bias pressure dipole over the Pacific between 0° and 30°S (10°N and 20°S) in summer (winter), which causes bias westerly/northwesterly winds off the Peruvian coast.

The reason for it remains unclear as does that for the warm bias during northern Argentinean austral summer. A full understanding of the latter would require further analyses of surface fluxes and atmospheric profiles, which are beyond the scope of this article.

3.2 Amazonia

In the following we focus on simulation results over Amazonia. Solman et al. (2013) have found most discrepancies between RCM simulations over this part of South America, which suggests a generally high modeling uncertainty in the region. Fortunately, all flux towers meeting the criteria mentioned in Sect. 2.3 are located in this area, so that we can compare modeled seasonal and diurnal cycles to site measurements. Further below in this section we present DJF statistics of different model variables over Amazonia, which is defined as a lat/lon box from 0° to 10°S and 50° to 70°W (Fig. 1).

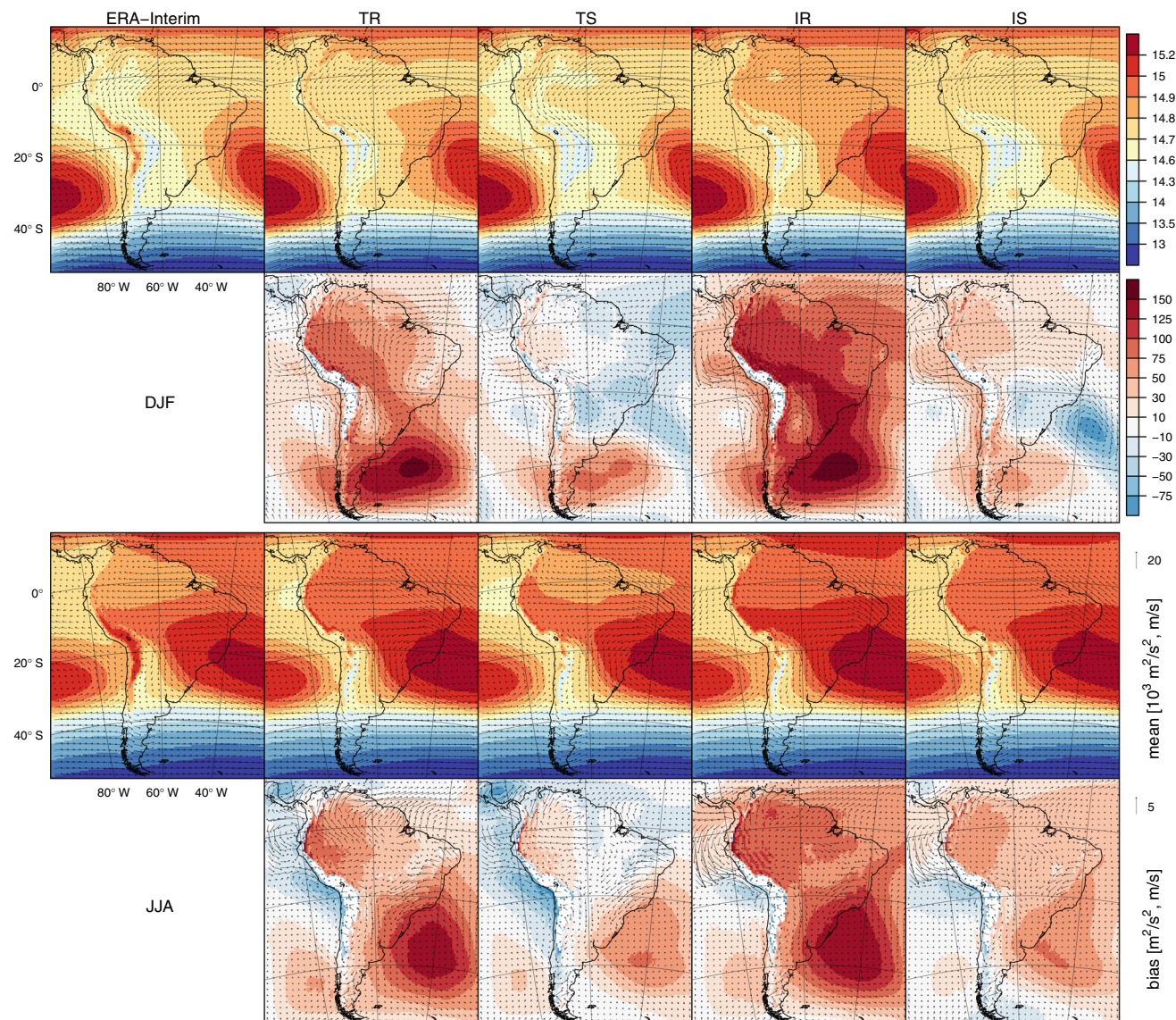


Fig. 7 Mean fields of geopotential height (colors) and wind (vectors) at 850 hPa versus ERA-Interim reanalyses from 1998 to 2011. Layout as described in Fig. 3

3.2.1 Seasonal cycles

We start with the seasonal cycles of precipitation, net surface radiation, and the 2 m temperature at the five flux tower sites (Fig. 8, Table 2). In order to assess measurement uncertainties we include cycles from the gridded datasets TRMM, SRB, and CRU as they were used for the evaluation of seasonal mean values above.

While the TRMM and SRB estimates mostly agree with the tower measurements, we find substantial differences between observed temperatures. The tower top temperatures are systematically lower than those estimated by the

CRU. The greater measurement height of 40–60 m of the towers alone cannot explain the differences of typically 1 to 2 °C. We presume that they are mainly due to the different meteorological conditions above a closed rainforest canopy, as represented by the tower measurements, and at a regular rainforest weather station, as represented by the CRU data. The fact that differences are smaller in dry than in wet season supports this presumption. Since modeled 2 m temperatures represent values above vegetation, the tower top data are the more suitable reference. This implies that the Amazonian cold bias diagnosed in Sect. 3.1.5 is at least less severe or even negligible, especially during wet season.

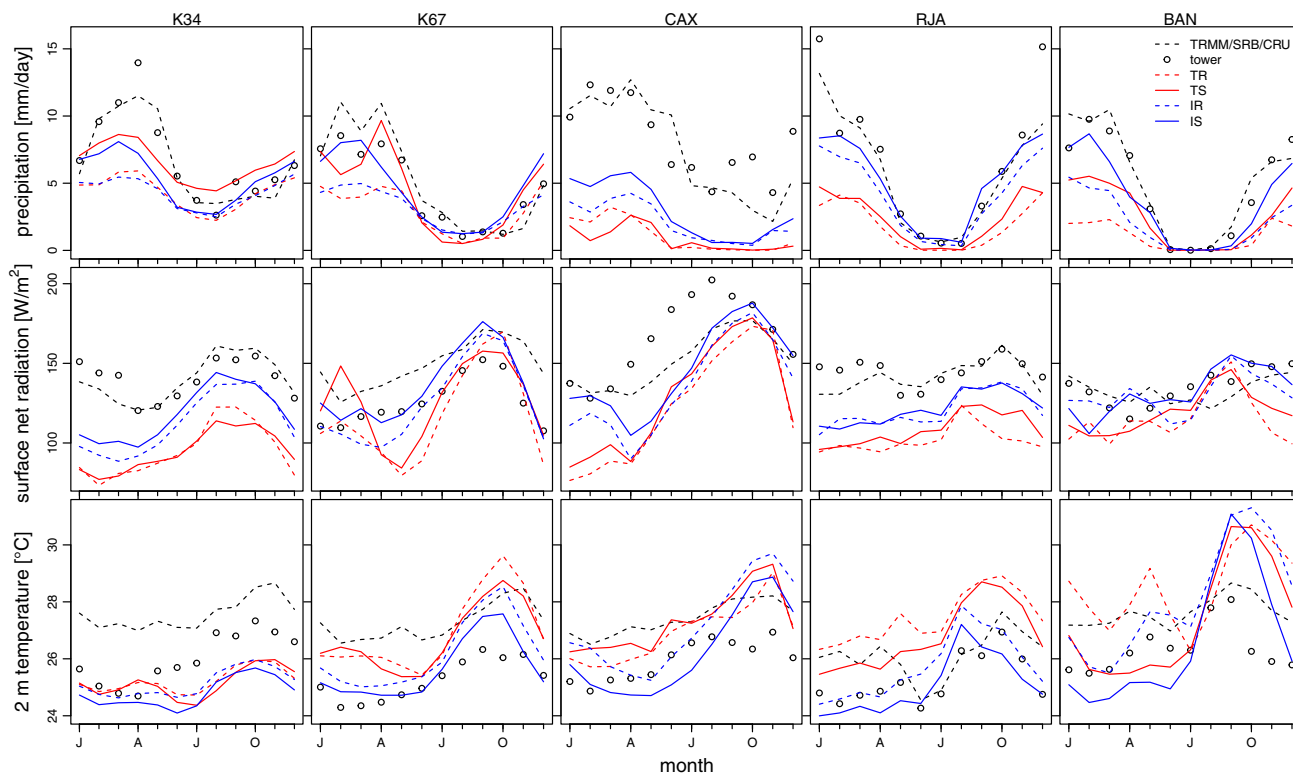


Fig. 8 Mean seasonal cycles of precipitation (*top row*), net surface radiation (*middle row*), and 2 m temperature (*bottom row*) modeled by the CCLM with four different setups (Table 3) versus

measurements at the five LBA flux tower sites (*columns*, Table 2). Also included are cycles from the gridded datasets TRMM, SRB, and CRU for precipitation, radiation, and temperature, respectively

In the following we discuss the results for each site individually, as measured cycles as well as model biases vary considerably between them.

Among the five towers, the K34 tower is the most centrally located in the Amazon basin. Together with the CAX site it has the least pronounced dry season with monthly mean precipitation rates remaining above 3 mm/day throughout the year; the rain peak is in MAM. Both characteristics are reproduced by all CCLM simulations. The MAM rates are strongly underestimated by all simulations however, especially by TR and IR. The net surface radiation is underestimated with all model setups in all months and by up to 50 W/m² in JFM. The seasonal cycles of 2 m temperatures do never differ by more than 1 °C between setups, have too small amplitudes, and show an average underestimation of 1 °C.

At the K67 site, the seasonal cycles of all three variables are well captured with the IS setup, whereas with the other setups, the model is either too dry, too warm, or overestimates the net radiation’s interseasonal variability.

The CAX tower is located close to the Amazon Delta and we recognize the severe dry bias discussed in Sect. 3.1.1. It is common to all model setups as well as a strong underestimation of net radiation from April to

August. Note that according to the SRB data the latter problem is less significant. The discrepancy between ground measurement and satellite product might be due to the complex shape of the coastline, which is nearby and cannot be represented properly at 1° resolution. Temperatures differ by up to 2 °C between model setups with drier simulations being warmer. In SONDJ the model is too warm with all setups.

The rainforest around the RJA site is subject to a high amplitude seasonal cycle of precipitation with mean rates below 2 mm/day in JJA and at up to 15 mm/day in DJF. The rain peaks are underestimated with all model setups but apart from that the seasonal cycle is well captured by the IS simulation. Surface net radiation is underestimated with all model setups in all months. The temperature cycle is simulated well with the IS setup; with the others temperatures are overestimated by up to 2 °C.

The BAN site, situated in a transition region between rainforest and savanna, features the most pronounced dry season. With each setup, the model underestimates rainfall during the onset of the wet season, which results in temperature overestimations by 3 to 4 °C. Inter-setup differences are large for precipitation and, consequently, temperature.

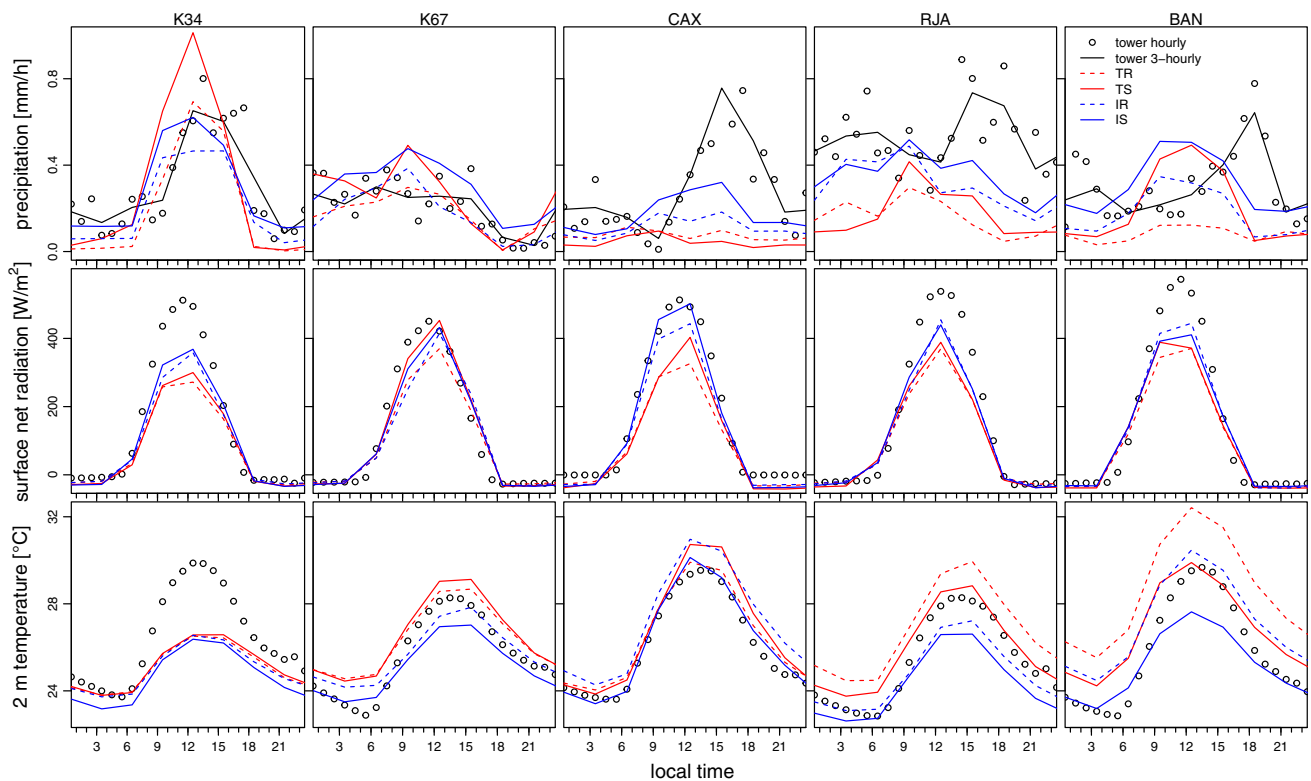


Fig. 9 Mean DJF diurnal cycles of precipitation, net surface radiation, and 2 m temperature, modeled by CCLM versus measured at the LBA flux towers. Layout as described in Fig. 8

In summary, we find a systematic underestimation of surface net radiation at the western sites K34 and RJA. As previously pointed out in Sect. 3.1.1, the model is not able to generate monthly mean rain rates of more than 10 mm/day over Amazonia. Temperatures show a strong response to precipitation at all sites subject to (simulated) dry stress. We do not see this response at the K34 site because here no simulation is dry enough to let soil moisture control evaporation rates (Koster et al. 2004) and in turn temperatures. The IS setup yields the best overall performance.

3.2.2 Diurnal cycles

In the following we focus on the austral summer since this is the wettest season at all flux tower sites except K34. The DJF diurnal cycles of precipitation, net surface radiation, and 2 m temperature are depicted in Fig. 9.

We observe that the underestimations of net surface radiation diagnosed before occur mainly at daytime. We find the strongest of those underestimations at the K34 site and see that it results in temperatures being 4 °C too low at noon. At all sites except CAX, the amplitude of the diurnal temperature cycle is too small for simulations with the IFS convection scheme.

However, the most striking deviations between modeled and measured diurnal cycles are found for precipitation. While CCLM simulates peak rain rates at noon or earlier at all sites, the measurements show them between 15 and 18 h local time—except at the K67 tower, where precipitation does not have a pronounced diurnal cycle. Especially at the CAX site there is a large difference between morning and afternoon rates which is not adequately captured by CCLM.

The problem of a proper representation of the diurnal cycle of convective precipitation over land is shared by various RCMs and GCMs (e.g., Dai et al. 1999; Betts and Jakob 2002; Grabowski et al. 2006; da Rocha et al. 2009; Nikulin et al. 2012). The reason for the too early precipitation peak was found to be a too easy triggering of moist convection by many convection schemes (Dai et al. 1999; Bechtold et al. 2004). Dai et al. (1999) conclude that “this keeps the model atmosphere from building up high CAPE and prevents intense precipitation from occurring.” Bechtold et al. (2014) show that slowing down the convective adjustment over tropical land can indeed lead to a higher buildup of CAPE prior to the onset of deep convection, which then occurs later and features greater peak rain rates. As these changes are shown to also result in enhanced mean precipitation, we think that CCLM’s inability to

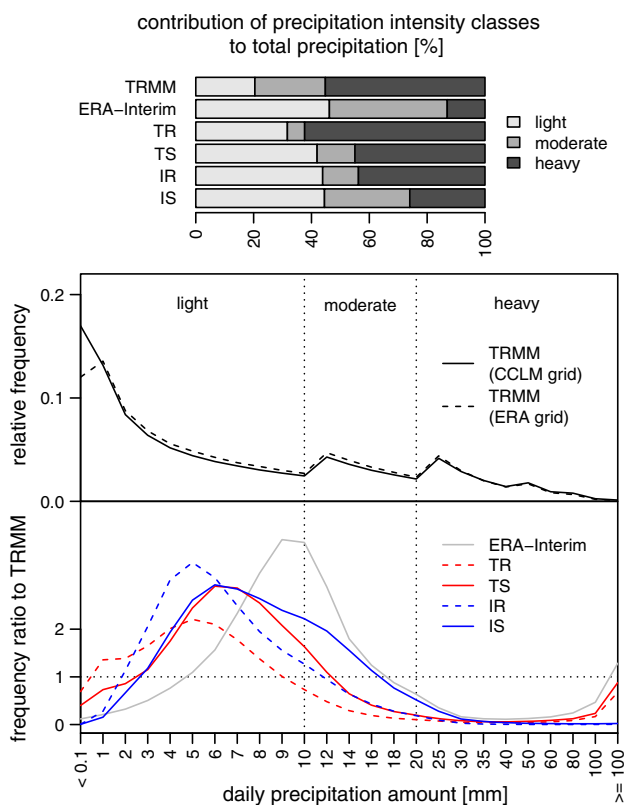


Fig. 10 Modeled and observed statistics of daily precipitation intensities over Amazonia in DJF from 1998 to 2011. *top* Relative contributions of daily precipitation amounts from different intensity classes to the total amount, with discrimination between light (<10 mm/day), moderate (10–20 mm/day), and heavy (>20 mm/day) precipitation events. *middle* Frequency distribution of daily rain amounts according to TRMM, interpolated to the CCLM and ERA-Interim grids. *bottom* Model-to-TRMM ratios of these frequencies for ERA-Interim and the four CCLM runs, with TRMM data interpolated to the respective grids

simulate monthly mean precipitation rates of more than 10 mm/day over Amazonia can be attributed to its poor representation of the diurnal cycle of convection.

Considering the diurnal and seasonal cycles of precipitation, net surface radiation, and 2 m temperature in synopsis, the model is most accurate at the K67 tower. According to Vera et al. (2006a, Fig. 5), occurrences of deep convective systems are rare around this site. This exemplifies that the model does fine where it does not need to simulate such systems.

3.2.3 Precipitation intensities

So far, we have only evaluated temporal mean rain amounts. When it comes to climate impacts, especially those of extreme events, there is yet another important characteristic of rainfall—the statistics of daily precipitation intensity. In the following, we evaluate two of these

statistics over Amazonia in DJF from 1998 to 2011 (Fig. 10).

CCLM and ERA-Interim show considerable biases in the frequency distribution of daily rain amounts. Both simulate too many wet days (>0.1 mm/day) and too infrequent heavy rain events (>20 mm/day), i.e. they rain a bit everyday instead of remaining dry on some days and raining fiercely on others. These problems are shared by many climate models (Dai 2006). Especially with the IFS convection scheme the underestimation of the number of days with less than 0.1 mm/day is dramatic.

ERA-Interim strongly overestimates the frequency of days with 5–15 mm precipitation. Depending on its setup, the CCLM produces too many days with precipitation between 1 to 9 (TR) and 3 to 17 (IS) mm/day. A swap of the subgrid-scale cloud scheme from RH to statistical moves the frequency distribution to higher intensities.

As a result of those differences, the contributions of light (<10 mm/day), moderate (10–20 mm/day), and heavy (>20 mm/day) rain events to precipitation totals vary across models and setups. According to the TRMM data, heavy rainfall should contribute 55 %, light and moderate rainfall only 20 and 25 %, respectively. In contrast to that, ERA-Interim and CCLM with the IS setup attribute the largest contribution to light precipitation with about 45 % and consequently underestimate the contribution of heavy rain events.

CCLM overestimates the contribution of light rainfall with the other setups as well, but that of heavy rainfall is estimated more properly. With the TR setup, heavy rainfall even contributes more than 60 % due to the very low total precipitation in combination with the simulation of some extreme events of more than 100 mm/day. Such extremes are only generated with the Tiedtke convection scheme. For a swap of the subgrid-scale cloud scheme from RH to statistical, we observe a favorable doubling of the contribution of moderate rain events to the total precipitation.

3.2.4 Cloud profiles

In Sect. 3.1 we have shown that simulations with the statistical subgrid-scale cloud scheme typically feature higher (lower) net surface shortwave (longwave) radiation than with the RH scheme. At daytime this sums up to a greater total net radiation (Fig. 9) which enables more vigorous convection and higher rain rates (Fig. 2, 9). We now want to illuminate how it is possible that the enhanced shortwave and reduced longwave net values coincide with an increased total cloud cover over Amazonia in DJF. To that end, the respective space-time averages of modeled vertical profiles of cloud cover C and convective cloud cover C_c [Eq. (1)] as well as specific cloud ice and liquid water contents are depicted in Fig. 11.

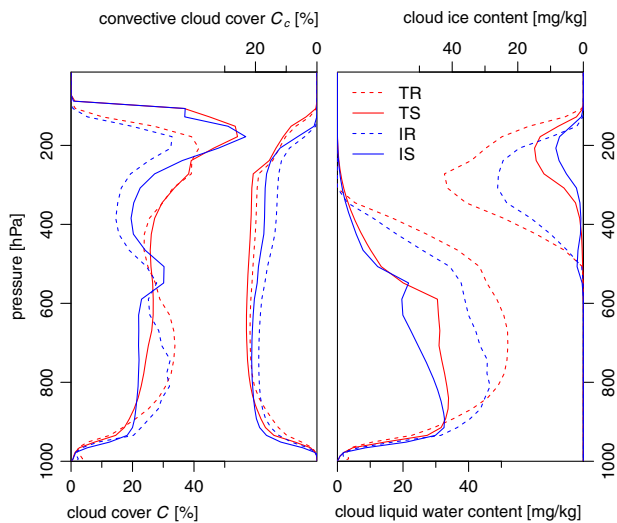


Fig. 11 Mean DJF vertical profiles of cloud cover C and convective cloud cover C_c [left, Eq. (1)] as well as specific cloud liquid water and ice contents (right) over Amazonia, as modeled with the four CCLM setups from 1998 to 2011

We observe that with the statistical scheme, on average, clouds contain 40 % less water and 75 % less ice than with the RH scheme. An analysis of the distribution of simulated stratiform cloud cover values reveals that this reduction is due to a practically complete disappearance of non-precipitating subgrid-scale clouds with the statistical scheme, i.e. with this scheme, all simulated clouds over Amazonia in DJF are either convective or grid-scale. In contrast, non-precipitating subgrid-scale clouds of both liquid water and ice do occur with the RH scheme, which leads to the respective increases in specific humidities.

A reduced cloud water content results in an atmosphere that is more translucent, the net surface shortwave radiation increases and more energy is available for buoyancy and convection. Consequently, we observe enhanced mean convective cloud cover values at all levels (Fig. 11) and greater mean rain rates (Fig. 2) with the statistical scheme.

Consistent with these changes we also find a marked increase of the mean high cloud cover (Fig. 11), probably due to more frequent occurrences of cirrus forming from the anvils of thunderstorm clouds. (Not shown: The Amazonian austral summer mean high cloud cover has a diurnal cycle that lags the convection cycle by about 4 hours and is strongly amplified with the statistical scheme.) This increase is the primary reason for the 5 to 15 % increase in DJF mean total cloud cover over Amazonia found in simulations with the statistical scheme (Fig. 3). Since high cirrus clouds are typically optically thin, their increased frequency of occurrence does not contradict a concurrently enhanced net surface shortwave radiation.

4 Conclusions

Our study provides a first in-depth evaluation of COSMO-CLM over South America. The analyses focus on precipitation, cloud cover, and surface net radiation. We compare the performances of the model with four different setups, which differ in the parametrizations of convection and subgrid-scale clouds.

The modeled climate is found to be highly sensitive to the parametrizations, particularly in tropical latitudes. While precipitation biases are large with the default Tiedtke convection and RH subgrid-scale cloud scheme, they can be strongly reduced employing the IFS convection and statistical subgrid-scale cloud scheme. With the latter setup, biases are within the range of those produced by other state-of-the-art RCM. COSMO-CLM is now ready for applications such as climate projections or the investigation of land use change scenarios for South America. Furthermore, our findings will help to improve the model's performance over other tropical domains.

Most tropical precipitation is convective and it is tempting to expect that its simulation is sensitive to the parametrization of convection. However, the sensitivity of modeled precipitation to the parametrization of subgrid-scale clouds turns out to be of similar magnitude. We explain this sensitivity with the surface radiation budget. With the statistical in place of the RH subgrid-scale cloud scheme, ice and liquid water contents of clouds are strongly reduced, which allows more solar radiation to reach the surface. As previously described by other authors, this allows for more vigorous convection and, in turn, enhanced precipitation rates.

For the variables considered in this study, the COSMO-CLM setup with the IFS convection and statistical subgrid-scale cloud scheme yields the best overall performance. Remaining model biases include an all-year dry bias over Amazonia with a pronounced land-sea bias contrast around the Amazon outlet. Low level pressure is generally overestimated over the tropical part of the continent. A substantial austral summer dry bias is present in northern Argentina and contributes to a pronounced warm bias found in the same region and season. Temperatures are generally too low in the tropics when compared to the CRU data. However, when considering the flux tower measurements this bias may be less distinct or even negligible in some cases.

Acknowledgments This paper was developed within the scope of the IRTG 1740/TRP 2011/50151-0, funded by the DFG/FAPESP. Map plots were made using the R package `ncdf4Utils` (Bhend and Rockel 2011). The authors appreciate observational data provision by the TRMM, ISCCP, NASA/GEWEX, CRU, ECMWF, and INPE/CPTEC. We thank Celso von Randow for his help on the flux tower data and Jürgen Kurths for his encouragement to write this paper.

Comments by two anonymous reviewers helped to improve the quality of the manuscript and are gratefully acknowledged.

References

- Avgoustoglou A (2011) Various Implementations of a Cloud Scheme in COSMO model. COSMO Newsletter 11, Deutscher Wetterdienst
- Baker IT, Prihodko L, Denning AS, Goulden M, Miller S, da Rocha HR (2008) Seasonal drought stress in the Amazon: reconciling models and observations. *J Geophys Res* 113(G1):G00B01. doi:10.1029/2007JG000644
- Bechtold P, Chaboureaud JP, Beljaars A, Betts AK, Köhler M, Miller M, Redelsperger JL (2004) The simulation of the diurnal cycle of convective precipitation over land in a global model. *Quart J Roy Meteor Soc* 130(604):3119–3137. doi:10.1256/qj.03.103
- Bechtold P, Köhler M, Jung T, Doblas-Reyes F, Leutbecher M, Rodwell MJ, Vitart F, Balsamo G (2008) Advances in simulating atmospheric variability with the ECMWF model: from synoptic to decadal time-scales. *Quart J Roy Meteor Soc* 134(634):1337–1351. doi:10.1002/qj.289
- Bechtold P, Semane N, Lopez P, Chaboureaud JP, Beljaars A, Bormann N (2014) Representing equilibrium and nonequilibrium convection in large-scale models. *J Atmos Sci* 71(2):734–753. doi:10.1175/JAS-D-13-0163.1
- Betts AK, Jakob C (2002) Evaluation of the diurnal cycle of precipitation, surface thermodynamics, and surface fluxes in the ECMWF model using LBA data. *J Geophys Res D Atmos* 107(D20):LBA 12-1–LBA 12-8. doi:10.1029/2001JD000427
- Bhend J, Rockel B (2011) ncd4Utils 0.5-1. <http://redc.clm-community.eu/projects/ncdf4Utils>
- Boers N, Bookhagen B, Marwan N, Kurths J, Marengo JA (2013) Complex networks identify spatial patterns of extreme rainfall events of the South American monsoon system. *Geophys Res Lett* 40:4386–4392
- Bookhagen B, Strecker MR (2008) Orographic barriers, high-resolution TRMM rainfall, and relief variations along the eastern Andes. *Geophys Res Lett* 35(6):L06403. doi:10.1029/2007GL032011
- Carvalho LMV, Jones C, Liebmann B (2004) The South Atlantic convergence zone: intensity, form, persistence, and relationships with intraseasonal to interannual activity and extreme rainfall. *J Clim* 17(1):88–108. doi:10.1175/1520-0442(2004)017<0088:TSACZI>2.0.CO;2
- Carvalho LMV, Jones C, Posadas AND, Quiroz R, Bookhagen B, Liebmann B (2012) Precipitation characteristics of the South American monsoon system derived from multiple datasets. *J Clim* 25(13):4600–4620. doi:10.1175/JCLI-D-11-00335.1
- Cook B, Zeng N, Yoon JH (2011) Will amazonia dry out? Magnitude and causes of change from IPCC climate model projections. *Earth Interact* 16(3):1–27. doi:10.1175/2011EI398.1
- Correia FWS, Alvalá RCS, Manzi AO (2008) Modeling the impacts of land cover change in Amazonia: a regional climate model (RCM) simulation study. *Theor Appl Climatol* 93(3–4):225–244. doi:10.1007/s00704-007-0335-z
- Dai A (2006) Precipitation characteristics in eighteen coupled climate models. *J Clim* 19(18):4605–4630. doi:10.1175/JCLI3884.1
- Dai A, Giorgi F, Trenberth KE (1999) Observed and model-simulated diurnal cycles of precipitation over the contiguous United States. *J Geophys Res D Atmos* 104(D6):6377–6402. doi:10.1029/98JD02720
- Davies HC (1976) A lateral boundary formulation for multi-level prediction models. *Quart J Roy Meteor Soc* 102(432):405–418. doi:10.1002/qj.49710243210
- Davin EL, Seneviratne SI (2011) Role of land surface processes and diffuse/direct radiation partitioning in simulating the European climate. *Biogeosci Dis* 8(6):11601–11630
- Dee DP, Uppala SM, Simmons AJ, Berrisford P, Poli P, Kobayashi S, Andrae U, Balmaseda MA, Balsamo G, Bauer P, Bechtold P, Beljaars ACM, van de Berg L, Bidlot J, Bormann N, Delsol C, Dragani R, Fuentes M, Geer AJ, Haimberger L, Healy SB, Hersbach H, Hólm EV, Isaksen L, Kållberg P, Köhler M, Matricardi M, McNally AP, Monge-Sanz BM, Morcrette JJ, Park BK, Peubey C, de Rosnay P, Tavolato C, Thépaut JN, Vitart F (2011) The ERA-Interim reanalysis: configuration and performance of the data assimilation system. *Quart J Roy Meteor Soc* 137(656):553–597. doi:10.1002/qj.828
- Dickinson R, Henderson-Sellers A, Kennedy P, Wilson M (1986) Biosphere-atmosphere transfer scheme (BATS) forcing the near community climate model. NCAR Technical Note TN275+STR, NCAR
- Dickinson RE (1984) Modeling Evapotranspiration for three-dimensional global climate models, vol 29, American Geophysical Union, pp 58–72. doi:10.1029/GM029p0058
- Doms G, Förstner J, Heise E, Herzog HJ, Mironov D, Raschendorfer M, Reinhardt T, Ritter B, Schrodin R, Schulz JP, Vogel G (2011) A Description of the Nonhydrostatic Regional COSMO Model. Physical Parameterization. Deutscher Wetterdienst, Part II
- Fischer EM, Beyerle U, Knutti R (2013) Robust spatially aggregated projections of climate extremes. *Nat Clim Change* 3(12):1033–1038
- Fischer T, Menz C, Su B, Scholten T (2013) Simulated and projected climate extremes in the Zhujiang River Basin, South China, using the regional climate model COSMO-CLM. *Int J Climatol* 33:2988–3001. doi:10.1002/joc.3643
- Garreaud RD, Vuille M, Compagnucci R, Marengo JA (2009) Present-day South American climate. *Palaeogeogr Palaeoclimatol* 281(3–4):180–195. doi:10.1016/j.palaeo.2007.10.032
- Geleyn JF, Hollingsworth A (1979) An economical analytical method for the computation of the interaction between scattering and line absorption of radiation. *Beitr Phys Atm* 52:1–16
- Giorgi F, Jones C, Asrar GR (2009) Addressing climate information needs at the regional level: the CORDEX framework. *WMO Bull* 58(3):175–183
- Grabowski WW, Bechtold P, Cheng A, Forbes R, Halliwell C, Khairoutdinov M, Lang S, Nasuno T, Petch J, Tao WK, Wong R, Wu X, Xu KM (2006) Daytime convective development over land: a model intercomparison based on LBA observations. *Quart J Roy Meteor Soc* 132(615):317–344. doi:10.1256/qj.04.147
- Gregory D, Morcrette JJ, Jakob C, Beljaars ACM, Stockdale T (2000) Revision of convection, radiation and cloud schemes in the ECMWF integrated forecasting system. *Quart J Roy Meteor Soc* 126(566):1685–1710
- Harris I, Jones PD, Osborn TJ, Lister DH (2013) Updated high-resolution grids of monthly climatic observations—the CRU TS3.10 Dataset. *Int J Climatol* in press. doi:10.1002/joc.3711
- Hohenegger C, Brockhaus P, Schar C (2008) Towards climate simulations at cloud-resolving scales. *Meteorol Z* 17(4):383–394. doi:10.1127/0941-2948/2008/0303
- Hohenegger C, Brockhaus P, Bretherton CS, Schär C (2009) The soil moisture-precipitation feedback in simulations with explicit and parameterized convection. *J Clim* 22(19):5003–5020. doi:10.1175/2009JCLI2604.1
- Huffman GJ, Bolvin DT, Nelkin EJ, Wolff DB, Adler RF, Gu G, Hong Y, Bowman KP, Stocker EF (2007) The TRMM multi-satellite precipitation analysis (TMPA): quasi-global, multiyear, combined-sensor precipitation estimates at fine scales. *J Hydrometeorol* 8(1):38–55. doi:10.1175/JHM560.1
- Jaeger EB, Anders I, Lüthi D, Rockel B, Schär C, Seneviratne SI (2008) Analysis of ERA40-driven CLM simulations for Europe. *Meteorol Z* 17(4):349–367. doi:10.1127/0941-2948/2008/0301

- Joetzjer E, Douville H, Delire C, Ciais P (2013) Present-day and future Amazonian precipitation in global climate models: CMIP5 versus CMIP3. *Clim Dyn* 41(11–12):2921–2936. doi:[10.1007/s00382-012-1644-1](https://doi.org/10.1007/s00382-012-1644-1)
- Jones PW (1999) First- and second-order conservative remapping schemes for grids in spherical coordinates. *Mon Weather Rev* 127(9):2204–2210. doi:[10.1175/1520-0493\(1999\)127<2204:fasocr>2.0.co;2](https://doi.org/10.1175/1520-0493(1999)127<2204:fasocr>2.0.co;2)
- Koster RD, Dirmeyer PA, Guo Z, Bonan G, Chan E, Cox P, Gordon CT, Kanae S, Kowalczyk E, Lawrence D, Liu P, Lu CH, Malyshev S, McAvaney B, Mitchell K, Mocko D, Oki T, Oleson K, Pitman A, Sud YC, Taylor CM, Verseghy D, Vasic R, Xue Y, Yamada T (2004) Regions of strong coupling between soil moisture and precipitation. *Science* 305(5687):1138–1140. doi:[10.1126/science.1100217](https://doi.org/10.1126/science.1100217)
- Liebmann B, Camargo SJ, Seth A, Marengo JA, Carvalho LMV, Allured D, Fu R, Vera CS (2007) Onset and end of the rainy season in south america in observations and the ECHAM 4.5 atmospheric general circulation model. *J Clim* 20(10):2037–2050. doi:[10.1175/JCLI4122.1](https://doi.org/10.1175/JCLI4122.1)
- Liersch S, Cools J, Kone B, Koch H, Diallo M, Reinhardt J, Fournet S, Aich V, Hattermann FF (2012) Vulnerability of rice production in the inner niger delta to water resources management under climate variability and change. *Environ Sci Policy* 34:18–33. doi:[10.1016/j.envsci.2012.10.014](https://doi.org/10.1016/j.envsci.2012.10.014)
- Marengo JA, Soares WR, Saulo C, Nicolini M (2004) Climatology of the low-level jet east of the Andes as derived from the ncep-ncar reanalyses: characteristics and temporal variability. *J Clim* 17(12):2261–2280. doi:[10.1175/1520-0442\(2004\)017<2261:COTLJE>2.0.CO;2](https://doi.org/10.1175/1520-0442(2004)017<2261:COTLJE>2.0.CO;2)
- Marengo JA, Jones R, Alves LM, Valverde MC (2009) Future change of temperature and precipitation extremes in South America as derived from the PRECIS regional climate modeling system. *Int J Climatol* 29(15):2241–2255. doi:[10.1002/joc.1863](https://doi.org/10.1002/joc.1863)
- Marengo JA, Ambrizzi T, da Rocha R, Alves L, Cuadra S, Valverde M, Torres R, Santos D, Ferraz S (2010) Future change of climate in South America in the late twenty-first century: intercomparison of scenarios from three regional climate models. *Clim Dyn* 35:1073–1097. doi:[10.1007/s00382-009-0721-6](https://doi.org/10.1007/s00382-009-0721-6)
- Marengo JA, Chou SC, Kay G, Alves LM, Pesquero JF, Soares WR, Santos DC, Lyra AA, Sueiro G, Betts R, Chagas DJ, Gomes JL, Bustamante JF, Tavares P (2012) Development of regional future climate change scenarios in South America using the Eta CPTEC/HadCM3 climate change projections: climatology and regional analyses for the Amazon, São Francisco and the Paraná River basins. *Clim Dyn* 38(9–10):1829–1848. doi:[10.1007/s00382-011-1155-5](https://doi.org/10.1007/s00382-011-1155-5)
- Marengo JA, Liebmann B, Grimm AM, Misra V, Cavalcanti IFA, Carvalho LMV, Berbery EH, Ambrizzi T, Vera CS, Saulo AC, Nogue-Paegle J, Zipser E, Seth A, Alves LM (2012) Recent developments on the South American monsoon system. *Int J Climatol* 32(1):1–21. doi:[10.1002/joc.2254](https://doi.org/10.1002/joc.2254)
- Mechoso CR, Robertson AW, Ropelewski CF, Grimm AM (2005) The American Monsoon Systems. In: *The Global monsoon system: research and forecast: report of the International Committee of the Third International Workshop on Monsoons (IWM-III)* 2–6, WMO
- Mellor GL (1977) The gaussian cloud model relations. *J Atmos Sci* 34(2):356–358. doi:[10.1175/1520-0469\(1977\)034<0356:TGCMR>2.0.CO;2](https://doi.org/10.1175/1520-0469(1977)034<0356:TGCMR>2.0.CO;2)
- Mellor GL, Yamada T (1982) Development of a turbulence closure model for geophysical fluid problems. *Rev Geophys* 20(4):851–875. doi:[10.1029/RG020i004p00851](https://doi.org/10.1029/RG020i004p00851)
- Mendes D, Souza EP, Marengo JA, Mendes MCD (2010) Climatology of extratropical cyclones over the South American-southern oceans sector. *Theor Appl Climatol* 100(3–4):239–250. doi:[10.1007/s00704-009-0161-6](https://doi.org/10.1007/s00704-009-0161-6)
- Molion LCB (1993) Amazonia rainfall and its variability, International Hydrology Series. Cambridge University Press, Cambridge
- Morcrette JJ, Barker HW, Cole JNS, Iacono MJ, Pincus R (2008) Impact of a new radiation package, McRad, in the ECMWF integrated forecasting system. *Mon Weather Rev* 136(12):4773–4798. doi:[10.1175/2008MWR2363.1](https://doi.org/10.1175/2008MWR2363.1)
- Nepstad DC, de Carvalho CR, Davidson EA, Jipp PH, Lefebvre PA, Negreiros GH, da Silva ED, Stone TA, Trumbore SE, Vieira S (1994) The role of deep roots in the hydrological and carbon cycles of Amazonian forests and pastures. *Nature* 372(6507):666–669. doi:[10.1038/372666a0](https://doi.org/10.1038/372666a0)
- Nicolini M, Salio P, Katzfey JJ, McGregor JL, Saulo AC (2002) January and July regional climate simulation over South America. *J Geophys Res D Atmos* 107(D22):ACL 12-1–ACL 12-13. doi:[10.1029/2001JD000736](https://doi.org/10.1029/2001JD000736)
- Nikulin G, Jones C, Giorgi F, Asrar G, Büchner M, Cerezo-Mota R, Christensen OB, Déqué M, Fernandez J, Hänsler A, van Meijgaard E, Samuelsson P, Sylla MB, Sushama L (2012) Precipitation climatology in an ensemble of CORDEX-Africa regional climate simulations. *J Clim* 25(18):6057–6078. doi:[10.1175/JCLI-D-11-00375.1](https://doi.org/10.1175/JCLI-D-11-00375.1)
- Nogués-Paegle J, Mechoso CR, Fu R, Berbery EH, Chao WC, Chen TC, Cook K, Diaz AF, Enfield D, Ferreira R, Grimm AM, Kousky V, Liebmann B, Marengo JA, Mo K, Neelin JD, Paegle J, Robertson AW, Seth A, Vera CS, Zhou J (2002) Progress in pan American CLIVAR research: understanding the South American monsoon. *Meteorologica* 27(1):3–32
- Panitz HJ, Dosio A, Büchner M, Lüthi D, Keuler K (2013) COSMO-CLM (CCLM) climate simulations over CORDEX-Africa domain: analysis of the ERA-Interim driven simulations at 0.44° and 0.22° resolution. *Clim Dyn*. doi:[10.1007/s00382-013-1834-5](https://doi.org/10.1007/s00382-013-1834-5)
- Parry ML, Canziani OF, Palutikof JP, van der Linder PJ, Hanson CE (2007) *Climate Change 2007: Impacts, Adaptation and Vulnerability*. Contribution of Working Group II to the Fourth Assessment Report of the Intergovernmental Panel on Climate Change, Cambridge University Press, Cambridge, UK, chap IPCC, 2007: Summary for Policymakers, pp 7–22
- Randall D, Khairoutdinov M, Arakawa A, Grabowski W (2003) Breaking the cloud parameterization deadlock. *Bull Am Meteorol Soc* 84(11):1547–1564. doi:[10.1175/BAMS-84-11-1547](https://doi.org/10.1175/BAMS-84-11-1547)
- Raschendorfer M (2001) The new turbulence parameterization of LM. COSMO Newsletter 1, Deutscher Wetterdienst
- Rickenbach TM, Ferreira RN, Halverson JB, Herdies DL (2002) Modulation of convection in the southwestern Amazon basin by extratropical stationary fronts. *J Geophys Res D Atmos* 107(D20):LBA 7-1–LBA 7-13. doi:[10.1029/2000JD000263](https://doi.org/10.1029/2000JD000263)
- Ritter B, Geleyn JF (1992) A comprehensive radiation scheme for numerical weather prediction models with potential applications in climate simulations. *Mon Weather Rev* 120(2):303–325. doi:[10.1175/1520-0493\(1992\)120<0303:ACRSFN>2.0.CO;2](https://doi.org/10.1175/1520-0493(1992)120<0303:ACRSFN>2.0.CO;2)
- da Rocha RP, Morales CA, Cuadra SV, Ambrizzi T (2009) Precipitation diurnal cycle and summer climatology assessment over South America: an evaluation of regional climate model version 3 simulations. *J Geophys Res D Atmos* 114(D10):D10108. doi:[10.1029/2008JD010212](https://doi.org/10.1029/2008JD010212)
- Rockel B, Geyer B (2008) The performance of the regional climate model CLM in different climate regions, based on the example of precipitation. *Meteorol Z* 17(4):487–498. doi:[10.1127/0941-2948/2008/0297](https://doi.org/10.1127/0941-2948/2008/0297)
- Rockel B, Will A, Hense A (2008) The regional climate model COSMO-CLM (CCLM). *Meteorol Z* 17(4):347–348. doi:[10.1127/0941-2948/2008/0309](https://doi.org/10.1127/0941-2948/2008/0309)

- Rosow WB, Schiffer RA (1999) Advances in understanding clouds from ISCCP. *Bull Am Meteorol Soc* 80(11):2261–2287. doi:[10.1175/1520-0477\(1999\)080<2261:AIUCFI>2.0.CO;2](https://doi.org/10.1175/1520-0477(1999)080<2261:AIUCFI>2.0.CO;2)
- Salazar LF, Nobre CA, Oyama MD (2007) Climate change consequences on the biome distribution in tropical South America. *Geophys Res Lett* 34(9):L09708. doi:[10.1029/2007GL029695](https://doi.org/10.1029/2007GL029695)
- Saleska SR, da Rocha HR, Huete AR, Nobre AD, Artaxo P, Shimabukuro YE (2009) LBA-ECO CD-32 Brazil Flux Network Integrated Data: 1999–2006. Data set. Available on-line: [<http://www.daac.ornl.gov>] from Oak Ridge National Laboratory Distributed Active Archive Center, Oak Ridge, Tennessee, USA and [<http://lba.cptec.inpe.br/>] from LBA Data and Information System, National Institute for Space Research (INPE/CPTEC), Cachoeira Paulista, Sao Paulo, Brazil
- Salio P, Nicolini M, Zipser EJ (2007) Mesoscale convective systems over southeastern South America and their relationship with the South American low-level jet. *Mon Weather Rev* 135(4):1290–1309. doi:[10.1175/MWR3305.1](https://doi.org/10.1175/MWR3305.1)
- Schewe J, Heinke J, Gerten D, Haddeland I, Arnell NW, Clark DB, Dankers R, Eisner S, Fekete BM, Colón-González FJ, Gosling SN, Kim H, Liu X, Masaki Y, Portmann FT, Satoh Y, Stacke T, Tang Q, Wada Y, Wisser D, Albrecht T, Frieler K, Piontek F, Warszawski L, Kabat P (2014) Multimodel assessment of water scarcity under climate change. *Proc Natl Acad Sci* 111(9):3245–3250. doi:[10.1073/pnas.1222460110](https://doi.org/10.1073/pnas.1222460110)
- Schrodin R, Heise E (2001) The multi-layer version of the DWD soil model TERRA-LM. COSMO Technical Report 2, Deutscher Wetterdienst
- Seth A, Rojas M (2003) Simulation and sensitivity in a nested modeling system for South America. Part I: reanalyses boundary forcing. *J Clim* 16(15):2437–2453
- Santos e Silva CM, de Freitas SR, Gielow R (2012) Numerical simulation of the diurnal cycle of rainfall in SW Amazon basin during the 1999 rainy season: the role of convective trigger function. *Theor Appl Climatol* 109(3–4):473–483. doi:[10.1007/s00704-011-0571-0](https://doi.org/10.1007/s00704-011-0571-0)
- Silva Dias MAF, Petersen W, Cifelli R, Betts AK, Longo M, Gomes AM, Fisch GF, Lima MA, Antonio MA, Albrecht RI (2002) A case study of convective organization into precipitating lines in the Southwest Amazon during the WETAMC and TRMM-LBA. *J Geophys Res D Atmos* 107(D20):LBA 46-1–LBA 46-23. doi:[10.1029/2001JD000375](https://doi.org/10.1029/2001JD000375)
- Slingo JM (1987) The development and verification of a cloud prediction scheme for the ecmwf model. *Quart J Roy Meteor Soc* 113(477):899–927. doi:[10.1002/qj.49711347710](https://doi.org/10.1002/qj.49711347710)
- Smagorinsky J (1960) On the dynamical prediction of large-scale condensation by numerical methods, *American Geophysical Union*, pp 71–78. doi:[10.1029/GM005p0071](https://doi.org/10.1029/GM005p0071)
- Solman SA, Sanchez E, Samuelsson P, Rocha RP, Li L, Marengo J, Pessacg NL, Remedio ARC, Chou SC, Berbery H, Treut H, Castro M, Jacob D (2013) Evaluation of an ensemble of regional climate model simulations over South America driven by the ERA-Interim reanalysis: model performance and uncertainties. *Clim Dyn* 41(5–6):1139–1157. doi:[10.1007/s00382-013-1667-2](https://doi.org/10.1007/s00382-013-1667-2)
- Sommeria G, Deardorff JW (1977) Subgrid-scale condensation in models of nonprecipitating clouds. *J Atmos Sci* 34(2):344–355. doi:[10.1175/1520-0469\(1977\)034<0344:SSCIMO>2.0.CO;2](https://doi.org/10.1175/1520-0469(1977)034<0344:SSCIMO>2.0.CO;2)
- Stackhouse PWJ, Gupta SK, Cox SJ, Mikovitz C, Zhang T, Hinkelman LM (2011) The NASA/GEWEX surface radiation budget release 3.0: 24.5-year dataset. *GEWEX News* 21(1):10–12, NASA
- Steppeleer J, Doms G, Schättler U, Bitzer HW, Gassmann A, Damrath U, Gregoric G (2003) Meso-gamma scale forecasts using the nonhydrostatic model LM. *Meteorol Atmos Phys* 82(1–4):75–96. doi:[10.1007/s00703-001-0592-9](https://doi.org/10.1007/s00703-001-0592-9)
- Stocker T, Qin D, Plattner GK, Tignor M, Allen SK, Boschung J, Nauels A, Xia Y, Bex V, Midgley PM (2013) *Climate Change 2013: The Physical Science Basis*. Contribution of Working Group I to the Fifth Assessment Report of the Intergovernmental Panel on Climate Change, Cambridge University Press, Cambridge, United Kingdom and New York, NY, USA, chap IPCC, 2013: Summary for Policymakers
- Taylor CM, de Jeu RAM, Guichard F, Harris PP, Dorigo WA (2012) Afternoon rain more likely over drier soils. *Nature* 489(7416):423–426. doi:[10.1038/nature11377](https://doi.org/10.1038/nature11377)
- Tiedtke M (1989) A comprehensive mass flux scheme for cumulus parameterization in large-scale models. *Mon Weather Rev* 117(8):1779–1800. doi:[10.1175/1520-0469\(2002\)059<1917:APPFTS>2.0.CO;2](https://doi.org/10.1175/1520-0469(2002)059<1917:APPFTS>2.0.CO;2)
- Tompkins AM (2002) A prognostic parameterization for the subgrid-scale variability of water vapor and clouds in large-scale models and its use to diagnose cloud cover. *J Atmos Sci* 59(12):1917–1942. doi:[10.1175/1520-0469\(2002\)059<1917:APPFTS>2.0.CO;2](https://doi.org/10.1175/1520-0469(2002)059<1917:APPFTS>2.0.CO;2)
- Toreti A, Naveau P, Zampieri M, Schindler A, Scoccimarro E, Xoplaki E, Dijkstra HA, Gualdi S, Luterbacher J (2013) Projections of global changes in precipitation extremes from coupled model intercomparison project phase 5 models. *Geophys Res Lett* 40(18):4887–4892. doi:[10.1002/grl.50940](https://doi.org/10.1002/grl.50940)
- Vera CS, Higgins W, Amador J, Ambrizzi T, Garreaud R, Gochis D, Gutzler D, Lettenmaier D, Marengo JA, Mechoso CR, Nogues-Paegle J, Dias PLS, Zhang C (2006) Toward a unified view of the American monsoon systems. *J Clim* 19(20):4977–5000. doi:[10.1175/JCLI3896.1](https://doi.org/10.1175/JCLI3896.1)
- Vera CS, Silvestri G, Liebmann B, González P (2006) Climate change scenarios for seasonal precipitation in South America from IPCC-AR4 models. *Geophys Res Lett* 33(13):L13707. doi:[10.1029/2006GL025759](https://doi.org/10.1029/2006GL025759)
- Žagar N, Andersson E, Fisher M (2005) Balanced tropical data assimilation based on a study of equatorial waves in ECMWF short-range forecast errors. *Quart J Roy Meteor Soc* 131(607):987–1011. doi:[10.1256/qj.04.54](https://doi.org/10.1256/qj.04.54)
- Žagar N, Skok G, Tribbia J (2011) Climatology of the ITCZ derived from ERA Interim reanalyses. *J Geophys Res D Atmos* 116(D15):D15103. doi:[10.1029/2011JD015695](https://doi.org/10.1029/2011JD015695)
- Wagner S, Fast I, Kaspar F (2011) Climatic changes between 20th century and pre-industrial times over South America in regional model simulations. *Clim Past Discuss* 7(5):2981–3022. doi:[10.5194/cpd-7-2981-2011](https://doi.org/10.5194/cpd-7-2981-2011)
- Warszawski L, Friend A, Ostberg S, Frieler K, Lucht W, Schaphoff S, Beerling D, Cadule P, Ciais P, Clark DB, Kahana R, Ito A, Keribin R, Kleidon A, Lomas M, Nishina K, Pavlick R, Rademacher TT, Buechner M, Piontek F, Schewe J, Serdeczny O, Schellnhuber HJ (2013) A multi-model analysis of risk of ecosystem shifts under climate change. *Environ Res Lett* 8(4). doi:[10.1088/1748-9326/8/4/044018](https://doi.org/10.1088/1748-9326/8/4/044018)
- Xu J, Small EE (2002) Simulating summertime rainfall variability in the North American monsoon region: the influence of convection and radiation parameterizations. *J Geophys Res D Atmos* 107(D23):ACL 22-1–ACL 22-17. doi:[10.1029/2001JD002047](https://doi.org/10.1029/2001JD002047)
- Zahn M, von Storch H (2008) A long-term climatology of North Atlantic polar lows. *Geophys Res Lett* 35(22). doi:[10.1029/2008GL035769](https://doi.org/10.1029/2008GL035769)
- Zhou J, Lau KM (1998) Does a monsoon climate exist over South America? *J Clim* 11(5):1020–1040. doi:[10.1175/1520-0442\(1998\)011<1020:DAMCEO>2.0.CO;2](https://doi.org/10.1175/1520-0442(1998)011<1020:DAMCEO>2.0.CO;2)